Journal of Physical and Chemical Reference Data

A Database of Experimentally Derived and Estimated Octanol–Air Partition Ratios (K_{0A})

Cite as: J. Phys. Chem. Ref. Data **50**, 043101 (2021); https://doi.org/10.1063/5.0059652
Submitted: 10 June 2021 • Accepted: 20 August 2021 • Published Online: 05 October 2021

Sivani Baskaran, Ying Duan Lei and Frank Wania

Journal of Physical and Chemical Reference Data | ARTICLE | scitation.org/journal/jpr

A Database of Experimentally Derived and Estimated Octanol–Air Partition Ratios (K_{OA})

Cite as: J. Phys. Chem. Ref. Data 50, 043101 (2021); doi: 10.1063/5.0059652
Submitted: 10 June 2021 • Accepted: 20 August 2021 •
Published Online: 5 October 2021

View Online Export Citation CrossMark

Sivani Baskaran, Ying Duan Lei, and Frank Wania[a)]

AFFILIATIONS

Department of Chemistry and Department of Physical and Environmental Sciences, University of Toronto Scarborough, Toronto, Ontario M1C 1A4, Canada

[a)]Author to whom correspondence should be addressed: frank.wania@utoronto.ca

ABSTRACT

Equilibrium partition coefficients or partition ratios are a fundamental concept in physical chemistry, with wide applications in environmental chemistry. While comprehensive data compilations for the octanol–water partition ratio and the Henry's law constant have existed for many years, no comparable effort for the octanol–air partition ratio (K_{OA}) exists. Considering the increasing use of K_{OA} in understanding a chemical's partitioning between a wide variety of organic phases (organic phases in atmospheric particles, plant foliage, polymeric sorbents, soil organic matter, animal tissues, etc.) and the gas phase, we have compiled all K_{OA} values reported in the published literature. The dataset includes more than 2500 experimentally derived values and more than 10 000 estimated values for K_{OA}, in total covering over 1500 distinct molecules. The range of measured $\log_{10} K_{OA}$ values extends from −2 to 13. Many more measured values have been reported in the $\log_{10} K_{OA}$ range from 2 to 5 and from 6 to 11 compared to the range from 5 to 6, which is due to the complementary applicability range of static and dynamic measurement techniques. The compilation also identifies measured data that are judged not reliable. K_{OA} values for substances capable of undergoing strong hydrogen bonding derived from regressions with retention times on nonpolar gas chromatographic columns deviate strongly from values estimated by prediction techniques that account for such intermolecular interactions and should be considered suspect. It is hoped that the database will serve as a source for locating existing K_{OA} data and for the calibration and evaluation of new K_{OA} prediction techniques.

Key words: database; octanol–air partition coefficient; partitioning; partition ratio; temperature.

CONTENTS

List of Tables

List of Figures

1. Introduction

Understanding the affinity of a chemical for liquid octanol, liquid water, and the gas phase is often the first step to understanding its potential environmental and biological fate and behavior. The physical–chemical properties to quantify those affinities include equilibrium partition ratios, saturation solubilities, and vapor pressure, which are related to one another through a series of thermodynamic triangles (Fig. 1). Chemical equilibrium partition ratios, hereafter simply referred to as partition ratios, are a concept fundamental to physical chemistry, with many applications in the fields of environmental, medicinal, and pharmaceutical sciences. While in the literature the thermodynamic property is more commonly referred to as a partition coefficient, we follow IUPAC nomenclature guidelines and describe the distribution of a chemical between two phases at equilibrium as a partition ratio.

The unitless octanol–air partition ratio (K_{OA}) describes the distribution of a chemical between octan-1-ol (CAS No. 111-87-5) and the gas phase at equilibrium,

$$K_{OA} = C_O/C_A, \tag{1}$$

where C_O and C_A are the concentrations of a compound in n-octanol and the gas phase in mol m^{-3}, respectively. K_{OA} has many possible applications, most notably in linear free–energy relationships

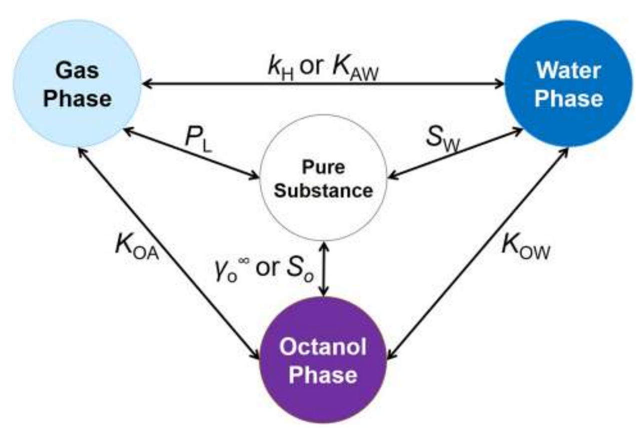

FIG. 1. Thermodynamic triangles of physical–chemical properties relating solvation in octanol, water, and in the pure liquid with the gas phase.

for predicting the equilibrium distribution of compounds between the gas phase and atmospheric particles (Finizio *et al.*, 1997), blood (Batterman *et al.*, 2002), soil (Hippelein and McLachlan, 2000; 1998), foliage (Müller *et al.*, 1994; Paterson *et al.*, 1990), and some of the polymers used in passive air samplers (Ockenden *et al.*, 1998; Shoeib and Harner, 2002a).

Many comprehensive reviews (Mackay *et al.*, 2015) and databases of octanol–water partition ratios (K_{OW}) (Leo *et al.*, 1971), Henry's law constants (k_H) (Mackay and Shiu, 1981; Sander 2015), and other physical–chemical properties [e.g., Mackay *et al.* (2006); Rumble *et al.* (2019); US EPA (2012)] exist in the literature. While Jin *et al.* (2017) compiled K_{OA} data for the development of an estimation model, there has been no comprehensive collection or review of K_{OA} data to date. Our aim is to assemble comprehensively and critically all previously published experimental and estimated K_{OA} data. This work further includes an overview of the different techniques that have been used to obtain K_{OA} values. The assembled database should be an easy-to-look-up repository of existing K_{OA} data but also be suitable for evaluating existing K_{OA} prediction techniques and the development of new ones.

1.1. Reporting K_{OA} values

In this section, we briefly review the various ways in which K_{OA} has been reported in the literature. In most cases, the values included in the database were reported as K_{OA} or $\log_{10} K_{OA}$ values; however, 1409 values were derived from reported Ostwald coefficients in octanol (L_{oct}), Henry's law constants in octanol (k_H^{oct}, Pa m^3 mol^{-1}), the Gibbs energies of dissolution into octanol from the gas phase (ΔG°, J mol^{-1}), or activity coefficients of a chemical in octanol at infinite dilution (γ_o^∞). While various papers report values using different units for pressure, temperature, and volume, we have reported all equations and variables using SI units (e.g., Pa for pressure, K for temperature, and m^3 for volume) unless otherwise stated.

1.1.1. Ostwald coefficient in octanol (L_{oct})

The earliest measurement of the solvation of a compound in octan-1-ol from the gas phase that we found was published in 1960 and was reported as an Ostwald coefficient in octanol (L_{oct}) by Boyer and Bircher (1960). The Ostwald coefficient has been used for over a century to describe the solubility of gases in liquids (Ostwald, 1891). Since Ostwald initially coined the term, the following definitions for the Ostwald coefficient at equilibrium have been used (Battino, 1984):

(i) L_V^0 is the volume of gas (V_G) dissolved in a volume of pure liquid (V_L^0),

$$L_V^0 = V_G/V_L^0, \tag{2}$$

(ii) L_V is the volume of gas (V_G) dissolved in a volume of solution (V_L),

$$L_V = V_G/V_L, \tag{3}$$

(iii) L_C represents the concentration of a gas in the liquid phase (C_L) divided by its concentration in the vapor phase (C_V),

$$L_C = C_L/C_V, \tag{4}$$

and

(iv) L_C^∞ is L_C at the infinite-dilution concentration of the gas in the liquid,

$$L_C^\infty = \lim_{C_L \to 0}(C_L/C_V). \tag{5}$$

Battino (1984) reviews more comprehensively the differences between these definitions and judges concentration-based definitions for equilibrium ratios to be the most thermodynamically reliable and useful method for reporting Ostwald coefficients (Battino, 1984; Wilhelm and Battino, 1985). The use of L_{oct} to describe octanol–air partitioning is not altogether common and is to our knowledge limited to Boyer and Bircher (1960), Wilcock *et al.* (1978), Pollack *et al.* (1984), and Bo *et al.* (1993). Unless the reference states otherwise, we assume all published L_{oct} values to be concentration ratios, equivalent to the K_{OA} value (Abraham *et al.*, 2001).

1.1.2. Gibbs energy (ΔG°_{oct})

The Gibbs energy describing the energy required to transfer a solute between two phases can also be expressed in two ways (Schwarzenbach *et al.*, 2005). If the Gibbs energy for octanol–air transfer is reported on a concentration basis (ΔG°), we can directly solve for K_{OA} using

$$\ln K_{OA} = -\Delta G_O^\circ/(RT), \tag{6}$$

where R is the ideal gas constant (8.314 J K^{-1} mol^{-1}) and T is the absolute temperature (in K). If the Gibbs energy is reported using partial pressure and mole fraction (ΔG^*), a conversion to ΔG° is first required (Berti *et al.*, 1986; Cabani *et al.*, 1991),

$$\Delta G_O^\circ = \Delta G_O^* - RT \cdot \ln(RT/v_{oct}), \tag{7}$$

where v_{oct} is the molar volume of octanol (0.000 158 m^3 mol^{-1} at 25 °C) (Rumble *et al.*, 2019; Yaws, 2012).

1.1.3. Henry's law constant in octanol (k_H^{oct})

Air–water equilibrium is often expressed with the Henry's law constant (k_H) (Fig. 1), typically with units of Pa m^3 mol^{-1}. Likewise, partitioning between octanol and air can be described as the k_H in octanol (k_H^{oct}) with units of Pa m^3 mol^{-1}. Leng *et al.* (2015) and Roberts (2005) described octanol–air partitioning using the Henry's law solubility constant, the reciprocal of k_H^{oct} ($k_H'^{oct}$, mol m^{-3} Pa^{-1}). K_{OA} is obtained using

$$K_{OA} = k_H'^{oct} \cdot RT = \frac{RT}{k_H^{oct}}. \tag{8}$$

1.1.4. Activity coefficients (γ_o^∞) and liquid vapor pressures (P_L)

K_{OA} can be related to a chemical's solubility S_O (in units of mol m^{-3} octanol) or activity coefficient at infinite dilution γ_o^∞ (hereafter referred to as the activity coefficient) in octanol,

$$K_{OA} = \frac{S_O \cdot RT}{P_L} = \frac{RT}{v_{oct} \cdot \gamma_o^\infty \cdot P_L}, \quad (9)$$

where P_L is the liquid-phase vapor pressure (in Pa). A K_{OA} value can therefore be calculated from a reported activity coefficient γ_o^∞ using the thermodynamic triangle of Eq. (9) if the vapor pressure of the liquid solute P_L is available. For the purposes of this database, we include K_{OA} values calculated using Eq. (9) if γ_o^∞ and P_L were measured for the same system (Hussam and Carr, 1985) or if the P_L was used to derive γ_o^∞ (Bhatia and Sandler, 1995; Dallas and Carr, 1992; Fukuchi *et al.*, 2001; 1999; Tse and Sandler 1994). Chemicals for which the reported solubilities or activity coefficients and the vapor pressures derive from different studies are not currently included in the database of measured K_{OA} values.

1.1.5. K_{OA} and K'_{OA}

Using another thermodynamic triangle, K_{OA} can be related to the ratio of the octanol–water (K_{OW} in units of m^3 water m^{-3} octanol) and air–water partition ratios (K_{AW} in units of m^3 water m^{-3} air) or the Henry's law constant in water (k_H in units of Pa m^3 water mol^{-1}),

$$K'_{OA} = K_{OW}/K_{AW} = (K_{OW} \cdot RT)/k_H. \quad (10)$$

Because during a K_{OW} determination, water–saturated octanol is being equilibrated with octanol–saturated water, the thermodynamic triangle of Eq. (10) yields the partitioning ratio between water–saturated octanol (referred to occasionally as "wet" octanol) and the gas phase, which we call K'_{OA}. The presence of water in octanol may increase the octanol solubility of more hydrophilic chemicals and reduce the octanol solubility of more hydrophobic chemicals (Beyer *et al.*, 2002).

In most instances, the K_{OA} reported in the literature refers to the ratio of concentrations of a chemical in pure octanol and the gas phase at equilibrium. However, this is not always the case [e.g., Xu and Kropscott (2014; 2012)]. Therefore, we note within the database whether K_{OA} or K'_{OA} is reported.

1.1.6. Internally consistent K values

The thermodynamic constraints imposed on the partitioning properties by the four thermodynamic triangles displayed in Fig. 1 have been used to adjust properties that are subject to measurement errors to yield a set of properties, called final adjusted values (FAVs), that is internally consistent and, by inference, subject to reduced error (Beyer *et al.*, 2002). Those efforts also take into account the potential discrepancy between K_{OA} and K'_{OA}. Whereas FAVs for the K_{OA} of hexachlorocyclohexanes (Xiao *et al.*, 2004), other organochlorine pesticides (Shen and Wania, 2005), polycyclic aromatic hydrocarbons (Ma *et al.*, 2010), polybrominated diphenyl ethers (Wania and Dugani, 2003), polychlorinated biphenyls (Li *et al.*, 2003), polychlorinated dibenzo-p-dioxins and -furans (Åberg *et al.*, 2008), and volatile methylsiloxanes (Xu *et al.*, 2014) have been reported in the literature, this database does not include them.

1.2. Temperature dependence of K_{OA}

K_{OA} is often highly temperature dependent. At higher temperatures, the K_{OA} of a chemical will be lower, as it becomes more volatile; at low temperatures, K_{OA} is higher. As an example, Fig. 2 plots $\log_{10} K_{OA}$ of DDT (CAS No. 50-29-3) against reciprocal absolute temperature T, where K_{OA} spans multiple orders of magnitude over a 50 °C temperature range. The slope m of the linear regression between $\log_{10} K_{OA}$ and $1/T$ is related to the molar internal energy of octanol-to-air phase transfer (ΔU°_{OA}, J mol^{-1}),

$$\Delta U^\circ_{OA} = -m \cdot R \cdot \ln 10. \quad (11)$$

If ΔU°_{OA} is assumed to be constant over a small range of temperatures, the van't Hoff equation can be used to calculate the K_{OA} at different temperatures,

$$\log_{10} \frac{K_{OA} \text{ at } T_2}{K_{OA} \text{ at } T_1} = -\frac{\Delta U^\circ_{OA}}{R} \cdot \left(\frac{1}{T_2} - \frac{1}{T_1}\right) \cdot \log_{10} e, \quad (12)$$

$$\ln \frac{K_{OA} \text{ at } T_2}{K_{OA} \text{ at } T_1} = -\frac{\Delta U^\circ_{OA}}{R} \cdot \left(\frac{1}{T_2} - \frac{1}{T_1}\right). \quad (13)$$

Here, ΔU°_{OA} expresses the temperature dependence of a partition ratio with the gas phase if the abundance of the chemical in the gas phase is expressed using a volumetric concentration (Goss and Eisenreich, 1996; Atkinson and Curthoys, 1978). The molar enthalpy of solution in octanol from the gas phase (ΔH°_{OA}, J mol^{-1}) is used when the chemical's abundance in air is expressed as partial pressure. ΔU°_{OA} is related to ΔH°_{OA} as follows:

$$\Delta U^\circ_{OA} = \Delta H^\circ_{OA} + RT. \quad (14)$$

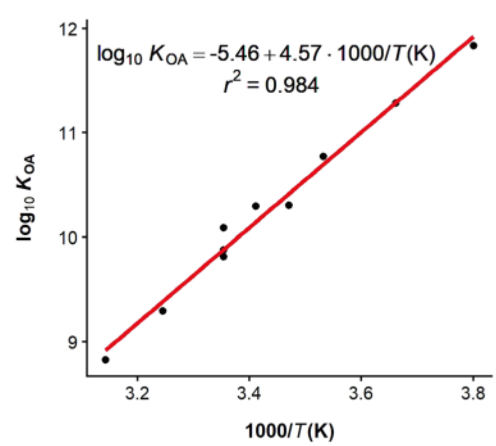

FIG. 2. Example of the temperature dependence of $\log_{10} K_{OA}$ for DDT (CAS No. 50-29-3) between −10 and 45 °C (Harner and Mackay, 1995; Shoeib and Harner, 2002b).

While K_{OA} is almost invariably reported on a volume basis, we found that in some instances ΔU°_{OA} has been mistakenly referred to as ΔH°_{OA}. We note the difference between the two variables because prediction techniques for ΔH°_{OA} (Mintz *et al.*, 2008; 2007) and direct measurements of ΔH°_{OA} using calorimetric techniques (Fuchs and Stephenson, 1985; Stephenson and Fuchs, 1985a; 1985b; 1985c; 1985d; 1985e) exist in the literature.

The ΔU°_{OA} must be negative because the slope m in Eq. (11) has a positive value (as $\log_{10} K_{OA}$ decreases with increasing temperature). Many papers report a positive ΔU°_{OA} value, which we believe to be ΔU°_{AO} values.

2. Experimental Techniques

The different experimental techniques used to measure $\log_{10} K_{OA}$ can be grouped into three broad categories: dynamic, static, and indirect. Many of the reported values are direct measurements made using the dynamic generator column technique or indirect measurements using gas chromatography retention time (GC-RT) methods. Dynamic techniques typically involve streaming air through or over a stationary octanol phase. In static measurement techniques, the octanol phase and air phase are in direct contact with each other in a closed vessel; however, neither phase is moving. Indirect techniques require a reference compound with a well-established measured K_{OA} value, and the elution time of the analyte relative to that of the reference compound is used to determine K_{OA}. In this section, we discuss each of these measurement techniques in greater detail. Table 1 summarizes the different techniques used to measure K_{OA}. Most techniques have a specific applicability range for K_{OA}. We also list the temperature range for these different measurements.

2.1. Static methods

In static techniques, either the gas phase, the octanol phase, or both are directly sampled and analyzed for the solutes once they have reached equilibrium within a closed system. This includes a variety of headspace techniques [e.g., Dallas (1995); Hussam and Carr (1985); Park *et al.* (1987); Treves *et al.* (2001); Xu and Kropscott (2014; 2013; 2012); and Lei *et al.* (2019)], a vacuum distillation method (Hiatt 1998; 1997), and a method based on measuring the kinetics of approaching an equilibrium distribution (Ha and Kwon 2010; Lee and Kwon 2016).

2.1.1. Headspace techniques

In the basic headspace technique, the solute is equilibrated between octanol and headspace in a closed container, whose temperature is controlled, for example, with a water bath. The concentration in the headspace is then quantified using gas chromatography and an external calibration. The concentration in octanol is determined by dissolving a known quantity of solute into a known volume of octanol, and the K_{OA} is then determined using Eq. (1). Headspace techniques can measure multiple solutes at the same time, at different temperatures, and at low solute concentrations.

Rohrschneider (1973) was one of the first to use headspace analysis to measure solvent–air interactions in many different solvents, including octanol. A small volume of solute was added to 2 ml of solvent and allowed to equilibrate for two to fifteen hours in a temperature bath. The headspace of the vial was sampled and calibrated against the response for the solute in a solvent for which K_{iA} is known (where i is a solvent).

The group of Carr *et al.* (Hussam and Carr, 1985; Park *et al.*, 1987; Dallas, 1995; and Castells *et al.*, 1999) refined the headspace technique for measuring solute partitioning between solvents and the gas phase. This technique has also been used by Cheong (1989), Abraham *et al.* (2001), and Dallas and Carr (1992). Typically, γ_o^{∞} and P_L are reported, allowing for K_{OA} to be derived using Eq. (9), or K_{OA} was reported directly. The data by Castells *et al.* (1999) are excluded from the database as no P_L values were reported.

Instead of a headspace vial, Xu and Kropscott (2013) used a 100 ml Hamilton syringe to equilibrate a solute between octanol and air. For analysis, air and octanol samples are taken through the same sampling port, with the former being collected onto a cold trap. A more complex apparatus involving two syringes connected by a small valve was used by Xu and Kropscott (2012) to simultaneously measure the partitioning equilibria between two solvents and the headspace. Using octanol saturated with water and water saturated with octanol as the two solvents, Xu and Kropscott (2012) measured the K'_{OA} with this system. While this technique can determine multiple phase equilibria of relatively volatile chemicals at the same time, it is extremely challenging to implement because all three phases need to be sampled quickly to avoid disturbing the equilibrium of the system.

The variable phase ratio headspace technique introduced by Ettre *et al.* (1993), and first applied to the measurement of K_{OA} by Lei *et al.* (2019), improves on the basic headspace technique by doing away with the need to quantify the solute concentration in the headspace. Variable volumes of the same octanol solution are placed into sealed vials and allowed to equilibrate. The reciprocal signal strength obtained from headspace analysis is regressed against the phase ratio, which is the volume of air to the volume of octanol solution present in each vial (Lei *et al.*, 2019). The K_{OA} is then determined as the intercept divided by the slope of the linear regression (Lei *et al.*, 2019), i.e., no calibration or quantification is required.

Whereas headspace techniques work well for volatile compounds, they are unsuitable for chemicals with $\log_{10} K_{OA}$ greater than about 4 (Lei *et al.*, 2019). One challenge of applying headspace techniques to less volatile solutes is that the concentrations in the headspace are often too small for reliable quantification. Treves *et al.* (2001) used solid-phase microextraction (SPME) fibers to collect the solute from the headspace and thus increase the amount delivered onto the GC column for analysis. A quantification of the headspace concentration, however, would require knowledge of a solute's gas–fiber partition ratio (K_{FG}) and a fiber-specific constant (k_F). Treves *et al.* (2001) eliminated the need to empirically determine K_{FG} and k_F of a chemical by using a reference compound with a known k_H. The response of each sample is plotted against the solution concentration, where the slope is equal to $K_{FG} \cdot k_F$ over $k_H^{oct} \cdot RT$.

Seeking to measure the partitioning of anesthetic gases between air and blood, Strum and Eger (1987) developed a headspace technique that can work with small amounts of solvent, which is particularly advantageous when working with human samples (e.g., blood).

TABLE 1. Summary of the different techniques used to obtain experimental K_{OA} values, including the K_{OA} and temperature ranges of the values reported in the database

Type of technique	Method	n	$\log_{10} K_{OA}$ range	Temperature range (°C)	References
Static	Headspace	196	−1.3–5.4	25–37	Abraham *et al.* (2001), Batterman *et al.* (2002), Cheong (1989), Dallas (1995), Dallas and Carr (1992), Hussam and Carr (1985), Park *et al.* (1987), and Rohrschneider (1973)
	Headspace with SPME	9	3.0–7.9	25	Treves *et al.* (2001)
	Headspace with syringe	93	−0.4–6.0	25	Eger *et al.* (1999; 1997), Fang *et al.* (1997a; 1997b; 1996), Ionescu *et al.* (1994), and Taheri *et al.* (1993; 1991)
	Variable phase ratio	78	1.6–4.4	25–110	Lei *et al.* (2019)
	Multiphase equilibrium	82	2.7–6.9	−5–40	Xu and Kropscott (2014; 2013; 2012)
	Droplet kinetics	18	5.4–11	25	Ha and Kwon (2010) and Lee and Kwon (2016)
	Vacuum distillation	121	0.5–5.6	25	Hiatt (1998; 1997)
	Gas solubility	45	−1.8–0.5	9–50	Bo *et al.* (1993), Boyer and Bircher (1960), Pollack *et al.* (1984), and Wilcock *et al.* (1978)
	Partial pressure	18	2.2–4.1	25	Berti *et al.* (1986) and Cabani *et al.* (1991)
Dynamic	Generator column or fugacity meter	745	4.0–12.6	−10–50	Dreyer *et al.* (2009), Goss *et al.* (2006), Harner *et al.* (2000), Harner and Bidleman (1998; 1996), Harner and Mackay (1995), Kömp and McLachlan (1997), Shoeib *et al.* (2004), Shoeib and Harner (2002b), Thuens *et al.* (2008), Wania *et al.* (2002), and Yao *et al.* (2007)
	Gas stripping	23	1.7–3.9	0–40	Fukuchi *et al.* (2001; 1999), Leng *et al.* (2015), and Roberts (2005)
	Dynamic gas–liquid chromatography retention time	96	1.6–3.9	20–50	Gruber *et al.* 1997
Indirect	Single reference, gas chromatography retention time	258	3.2–14	10–25	Lei *et al.* (2004), Odabasi *et al.* (2006a; 2006b), Odabasi and Cetin (2012), Okeme *et al.* (2020), Özcan (2013), Pegoraro *et al.* (2015), Vuong *et al.* (2020), Wang *et al.* (2017), Wania *et al.* (2002), Yaman *et al.* (2020), Zhang *et al.* (2009), and Zhao *et al.* (2010; 2009)
	Multi reference gas chromatography retention time	412	2.9–13.4	0–50	Shoeib and Harner (2002a), Su *et al.* (2002), and Zhang *et al.* (1999)
	Multi reference, single column, gas chromatography retention time	230	2.7–12.4	10–50	Su *et al.* (2002)
	Retention time index	46	8.4–13	7–25	Chen *et al.* (2001) and Harner *et al.* (2000)
	Gas–liquid chromatography retention time	47	1.9–3.6	25–50	Bhatia and Sandler (1995) and Tse and Sandler (1994)

This technique was widely used in the field of anesthesiology for a range of solvents. The technique as described by Taheri *et al.* (1991), and variations thereof, have been employed by Eger and colleagues to measure K_{OA} at 37 °C (Eger *et al.*, 1997; 2001; Fang *et al.*, 1997a; 1997b; 1996; Ionescu *et al.*, 1994; and Taheri *et al.*, 1993). A volume of the gaseous analyte is dissolved into octanol and the concentration of the solute in the headspace is determined using gas chromatography. A small aliquot of the octanol solution is then added to a larger evacuated flask. The pressure in the flask is slowly released, and a syringe is used to pump additional air to the system and mix the gaseous phase. The air in the syringe is then analyzed to determine the concentration of the solute in the gaseous phase. K_{OA} in this method is derived as a function of the volume of the flask, the volume of the aliquot of octanol solution in the flask, and the initial and final concentrations of the solute in the gas phase sampled above the octanol solution. This is a highly complex methodology and is therefore more likely to be prone to error. It is also limited to gaseous solutes, which must be available in a relatively pure form. These gaseous solutes will have low $\log_{10} K_{OA}$ values.

2.1.2. Vacuum distillation and gas chromatography

Hiatt reported K_{OA} values while working to improve upon earlier designs of a vacuum distillation with gas chromatography and mass spectrometry (VD/GC/MS) technique for quantifying volatile organic compounds (VOCs) in complex environmental matrices, such as fish tissue and vegetation (Hiatt, 1998; 1997). A sample and a spike containing the analytes of interest are placed in the sample chamber and allowed to equilibrate for three hours (Hiatt 1995). The sample chamber is then evacuated using a vacuum pump for five minutes, and the evacuated air passes first through a condenser column, to collect water vapor, and then a cryo-loop, submerged in liquid nitrogen, to collect the distillate (Hiatt, 1995). A carrier gas is then used to push the distillate through to a GC/MS for analysis (Hiatt, 1995). K_{OA} is then calculated based on the analyte recovery from the organic phase and a calculated K_{OA} of surrogate analytes (Hiatt, 1997). A major flaw of this measurement technique is the use of calculated K'_{OA} values for the surrogate analytes. The method also assumes that fish tissue and leaves are representative of pure octanol—however, we note that the values reported in these works are not explicitly indicated to be K_{OA} measurements. While the reverse can be used as an estimation technique, this assumption is not ideal for deriving physical–chemical properties of chemicals. Some of the reported K_{OA} values have a large degree of error (Hiatt, 1997).

2.1.3. Gas solubility techniques

Two general techniques were found to measure the L_{oct} of gaseous compounds. The first is used specifically for measuring the solubility of xenon (Xe, CAS No. 7440-63-3). Here, Pollack *et al.* (1984) used a NaI(Tl) crystal paired with a photomultiplier, which is directed at a fixed amount of gaseous Xe held within a sealed chamber (Pollack and Himm, 1982). The chamber is connected to a flask containing a known amount of solvent, in this case octanol, with some headspace (Pollack and Himm, 1982). The Xe is allowed to reach equilibrium with the solvent and excess gas. K_{OA} can be determined based on the volume of the gaseous phases in the two chambers and the volume of the solvent and by quantifying the amount of Xe present before and after equilibrium is reached (Pollack and Himm, 1982).

The second gas solubility technique often involves the use of specific equipment, such as the Van Slyke–Neill blood gas apparatus (Boyer and Bircher, 1960), modified Morrison–Billett apparatus (Wilcock *et al.*, 1978), or the Ben–Naim/Baer-type apparatus (Bo *et al.*, 1993). These techniques are scarcely described in the original literature; however, Battino and Clever (1966) described the technique using the Morrison–Billet apparatus and the Ben–Naim/Baer-type apparatus in an early review. An excess amount of gas is dissolved into a solvent and then the solution is degassed into an apparatus. The solvent is then saturated with the gas analyte at a constant temperature (Battino and Clever, 1966). Knowledge of the volume of the solvent in which the gas was dissolved and the pressure and volume of gas dissolved yields the gas solubility, and this combined with the partial pressure of the system can provide the L_{oct}.

2.1.4. Droplet kinetics

In the technique by Ha and Kwon (2010), a tiny droplet of octanol is suspended above an octanol solution within a sealed vial. The kinetics of uptake in the droplet of the solutes of interest and of a reference chemical with a well-established $\log_{10} K_{OA}$ is recorded by measuring the concentrations in the droplet after variable periods of time. The K_{OA} can then be derived from the kinetics of uptake if the thickness of the air boundary layer, the molecular diffusivity of the chemical in air, and the surface area and volume of the octanol droplet are known. The reference compound serves to calibrate the thickness of the air diffusive boundary layer. The K_{OA} of the analytes of interest must be sufficiently high so that the mass transfer resistance of the chemical in the octanol is negligible relative to that in air (Ha and Kwon 2010). The length of the experiment depends on the anticipated K_{OA} value, as it will take longer for a change in the chemical concentration in the octanol droplet to be quantifiable for chemicals with high $\log_{10} K_{OA}$ values (Ha and Kwon, 2010). Although their measurements were conducted at 25 °C, Ha and Kwon suggested that this method can be used to obtain K_{OA} at different temperatures, as long as the octanol drop does not evaporate (Ha and Kwon, 2010). This measurement technique is applicable to chemicals with a $\log_{10} K_{OA}$ between 5 and 9 (Ha and Kwon, 2010), i.e., it extends to higher values than are typically accessible with static headspace techniques.

2.1.5. Partial pressure

Measurements of the partial vapor pressure of solutes in octanol can be used to determine the ΔG° of solvation into octanol (Berti *et al.*, 1986; Cabani *et al.*, 1991). The vapor pressure of octanol is first determined using a static apparatus (Berti *et al.*, 1986). The partial pressure of the solute over solution is measured at varying molar ratios and is used to solve for $\Delta G'_{OA}$ (Berti *et al.*, 1986). By regressing the molar ratio with $\Delta G'_{OA}$, the authors extrapolated to solve for ΔG^{*}_{OA} where the pressure (in atm) and molar ratio are equal to 1 (Berti *et al.*, 1986). Equation (7) is then used to solve for ΔG°_{OA} (Berti *et al.*, 1986).

2.2. Dynamic methods

The challenge of static techniques for K_{OA} determination is that the amount of less volatile compounds in the gas phase is too small for reliable determination. It is therefore often necessary to greatly increase the volume of air that is being equilibrated with the octanol phase. If the determination is based on the amount of solute being lost from the octanol phase, it can also be beneficial to minimize the volume of octanol in the experimental system. Dynamic techniques for measuring K_{OA} involve passing a stream of air through or past a stationary octanol solution. Therefore, the volume of air can be increased by extending the length of time that the air is flowing past the octanol.

The generator column techniques require the amount of analyte transferred from octanol to the gas stream to be quantified, whereas in gas stripping techniques only the rate of change in the concentration of the analyte in the gas stream or the solvent must be recorded. In the dynamic gas–liquid chromatography technique, K_{OA} is derived from the time it takes for a chemical to travel through a gas chromatographic column with octanol as a stationary phase. The generator column technique is by far the most commonly applied dynamic method because it is one of the few techniques readily applicable to less volatile solutes.

2.2.1. Generator column or fugacity meter

The generator column technique, sometimes also referred to as the fugacity meter technique, involves passing large volumes of air through a stationary octanol phase. First used by Harner and Mackay (1995), this technique has since been used extensively in different configurations (Kömp and McLachlan, 1997; Dreyer *et al.*, 2009; etc.). Either glass wool or glass beads are coated with a small volume of an octanol solution and are placed in a column. Air passing through the column at a controlled rate for a measured length of time equilibrates with the octanol. The air is saturated with octanol prior to passage through the column to prevent the vaporization of octanol. The amount of chemical that partitions from the spiked octanol into the air phase is trapped and quantified to determine a concentration in air, C_A. Using the known concentration of the chemical in octanol, C_O, yields K_{OA} from Eq. (1).

This method requires the validity of several assumptions to yield reliable results. The concentration of the analytes of interest in the octanol needs to be sufficiently high to remain constant throughout the measurement. The flow rate must be sufficiently slow for the chemicals to reach equilibrium between octanol and air. The length of an experiment must balance the need to collect an amount of chemical from the air stream that is sufficient for reliable quantification but not so much that it would deplete the chemical from the spiked column.

2.2.2. Gas stripping and bubbling techniques

This technique is commonly applied for measuring k_H and involves passing air past a stationary solvent phase. Two variations of this technique have been applied to measuring K_{OA}.

Adopting the gas stripping method by Leroi *et al.* (1977), Fukuchi *et al.* (2001; 1999) moved small air bubbles through a very small volume of octanol containing the solute of interest. Equilibration is assured by a slow flow rate and small bubble size. A temperature bath allows for measurements at different temperatures. By recording the concentration change of the solute in the gas phase over time, Fukuchi *et al.* derived γ_o^∞ from the gas flow rate and the solute's estimated P_L. The volume of octanol is assumed to be constant (Leroi *et al.*, 1977). We used Eq. (9), the measured γ_o^∞, and the estimated P_L to derive the K_{OA} value. This technique has only been used for four ether compounds.

In the technique by Roberts (2005), the solute is not added directly to the octanol, but the gas is first bubbled through a small volume of the liquid solute prior to being bubbled through a volume of octanol. Once the solute has reached equilibrium between the gas and octanol, the gas concentration of the solute at the outlet will be constant. At this point, the solute is removed from the gas flow, and the gas begins to strip the octanol of any solute (Roberts, 2005). Measuring the change in the concentration of the solute at the outlet allows for the determination of a first-order rate loss constant for the chemical from octanol. When combined with the octanol volume and gas flow rate, K_{OA} can be obtained (Roberts, 2005). This technique has been applied to measure the K_{OA} of peroxyacetyl nitrate (CAS No. 2278-22-0) (Roberts, 2005) and triethylamine (CAS No. 121-44-8) (Leng *et al.*, 2015).

Among the advantages of the gas stripping techniques are that analysis of only one phase is required and that no quantification is necessary because the change in signal strength over time can be plotted in place of concentration. This also eliminates the need for a calibration curve. Finally, this technique uses multiple measurements to obtain a single K_{OA} value, which increases the reliability of the experimental value. However, solute volatility limits the applicability of gas stripping techniques to a fairly narrow range of K_{OA}. The technique employed by Roberts (2005) is also limited to liquid solutes.

2.2.3. Gas–liquid chromatography retention time

Some dynamic methods rely on the determination of the retention of a solute in a gas chromatographic column containing octanol as a stationary phase. No quantification of the amount of solute in either octanol or gas phase is necessary. The use of octanol as a stationary phase sets these methods apart from other retention time techniques using commercial columns, which rely on correlations and always require reference compounds with a known K_{OA}. They will be discussed in the next section.

Gruber *et al.* (1997) recorded the net retention volume (V_N) on columns with variable volumes of octanol (V_L) coated on the inside. When V_N/V_L is regressed against the reciprocal of V_L, the intercept yields K_{OA} (Gruber *et al.*, 1997). This technique has similarities with the static variable phase ratio technique by Lei *et al.* (2019) described above.

Sandler *et al.* (Tse and Sandler, 1994; Bhatia and Sandler, 1995) used a slightly different gas chromatographic method, relying on the use of a reference compounds with a known γ_o^∞ (hexane and heptane), to measure the γ_o^∞ of halogenated alkanes. The ratio of the elution time of the reference compound and the solutes of interest relative to that of methane is used, together with an estimated P_L. We utilize the reported γ_o^∞ and P_L to calculate K_{OA} using Eq. (9).

2.3. Indirect gas-chromatographic retention time methods

Indirect techniques seek to derive K_{OA} from the retention time of solutes on commercial gas chromatographic columns, i.e., the stationary phases of those columns serve as surrogates for the octanol phase. Because these surrogates are imperfect, indirect methods always require a calibration and often relate the retention times of the analytes of interest to those of reference compounds with previously measured K_{OA} values. There are a few variations of the gas chromatography retention time (GC-RT) technique; however, they all have in common that at least one chemical with a well-established K_{OA} value at different temperatures is required.

The first instance of measuring K_{OA} using GC-RT was by Zhang *et al.* (1999), who regressed capacity factors of chemicals on multiple columns with their K_{OA} to obtain a multiple linear regression (MLR) equation. The K_{OA} of multiple calibration chemicals need to be known as a function of temperature, as separate MLR equations are required for different temperatures. While the use of multiple columns with different solid phases is meant to better account for different types of interactions of a chemical with octanol (Zhang *et al.*, 1999), Su *et al.* (2002) showed that a linear regression with a single column's capacity factor worked equally well and yielded K_{OA} values with a smaller error.

The retention time index (RTI) method is essentially a technique for extrapolating known K_{OA} values within a group of structurally related compounds by linearly regressing directly determined $\log_{10} K_{OA}$ values against the compounds' RTI (Harner *et al.*, 2000). The RTI relates the retention time of the solute to that of linear alkanes. The regression equation is then used to estimate K_{OA} for other related compounds using their RTI. A separate regression for different experimental temperatures is required. By further regressing the slope and intercept of these linear regressions against temperature, the $\log_{10} K_{OA}$ at different temperatures can be determined solely from the RTI of a chemical. This method relies heavily on having direct measurements of K_{OA} at different temperatures for different congeners and RTI values for each congener. When applying this method to polychlorinated dibenzo-dioxins and -furans (PCDD/Fs), Harner *et al.* (2000) also accounted for the position and number of chlorine substitutions because measurements with the generator column technique had revealed that tetra-, penta-, and hexa- PCDD/Fs with 3-4 chlorines in the 2,3,7, and/or 8 positions had a higher affinity to the octanol phase (Harner *et al.*, 2000). This illustrates the need for good calibration and reference data when using indirect K_{OA} measurement techniques.

Adapting a technique for the determination of P_L, Wania *et al.* (2002) used the retention time of a chemical relative to a single reference chemical in order to obtain K_{OA}. In principle, the relative retention times of the analyte (t_{Ri}) and the reference compound (t_{Rref}) are proportional to the partition ratio between the stationary phase of the column and air, which is also proportional to K_{OA} (Wania *et al.*, 2002). Thus, this method only requires a single reference compound to have well established K_{OA} values at different temperatures. These $\log_{10} K_{OA}$ values are plotted against ln (t_{Ri}/t_{Rref}) to produce a linear regression with a slope equal to $\Delta U_{OAi}/\Delta U_{OAref} - 1$. The internal energy of octanol gas phase transfer ΔU_{OAi} then allows for the determination of K_{OA} at different temperatures (Wania *et al.*, 2002). The obtained K_{OA} values are then regressed against literature values of K_{OA} obtained using direct measurement techniques. Therefore, even though only one chemical is needed as a reference compound, calibration compounds with established K_{OA} values are needed to improve the reliability of the results. Wania *et al.* (2002) also showed the importance of selecting an appropriate reference compound because interactions of different compounds with the stationary phase and octanol may be dissimilar. This technique is the most commonly applied GC-RT for K_{OA} determination.

3. Estimation Techniques

Numerous techniques for estimating K_{OA} exist. We describe here a few of the major techniques if they had been specifically designed for estimating K_{OA} and if K_{OA} estimated with those techniques have been reported in the literature. If K_{OA} values had been calculated in the context of studies on passive air sampling, atmospheric particle–gas partitioning, or environmental fate modeling, they are not considered. Only articles focusing on physical–chemical property estimation techniques or work comparing experimental and/or estimated K_{OA} values are included within the database and in this review. Table 2 summarizes the different techniques for estimating K_{OA}. These techniques tend to have a wider applicability range than the experimental ones. We also list the temperature range for these methods. Most of the estimation models for K_{OA} are Quantitative Structure–Property Relationships (QSPRs). Density functional theory-based solvation models have also been used to determine K_{OA} by first obtaining ΔG°_{OA} of a chemical in octanol [see Eq. (6)].

3.1. QSPR techniques

QSPR techniques typically involve the regression of descriptors against the property of interest to obtain an equation of best fit that will most accurately predict K_{OA}. These models can be very simple, using basic thermodynamic relationships and linear regressions or using machine learning algorithms to estimate K_{OA} based on a series of chemical descriptors.

3.1.1. Thermodynamic triangles

K_{OA} can be derived from other properties using thermodynamic triangles [see Fig. 1 and Eqs. (9) and (10)]. The two property values used in such an estimation should ideally be experimentally derived. If they are themselves estimated values, the uncertainty of their prediction propagates to K_{OA}.

Most estimations of K_{OA} reported in the literature are derived using Eq. (10), using either experimental or estimated values of K_{OW} and K_{AW}. This can be a useful estimation method for chemicals with well-established K_{OW} and K_{AW} values. However, Finizio *et al.* (1997) already noted that six K_{OA} values estimated this way were between 0.48 and 1.04 $\log_{10}$ units smaller than experimental values, which may be related to the estimation yielding wet octanol–air partition ratio (K'_{OA}) (see Sec. 1.1.5). Meylan and Howard (2005) conducted the first comprehensive assessment of this technique for estimating K_{OA} using K_{OW} and K_{AW}. They also explored the temperature dependence of K_{OA} by combining a temperature-adjusted K_{AW} value with the K_{OW} of a chemical at 25 °C and using K_{AW} and K_{OW} values estimated with EPISuite^{TM}'s HENRYWIN and KOWWIN (Meylan and Howard, 2005). This estimation technique is what is used in the KOAWIN model included in EPISuite^{TM} (EPI Suite Data, 2012).

The use of Eq. (9) is less common but advantageous as it does not yield a K'_{OA} value. Abraham *et al.* (2001) presented the K_{OA} of some chemicals derived from measured P_L and S_O. Sepassi and Yalkowsky (2007) used P_L and S_O estimated from other physical–chemical properties of a compound, including boiling-point temperature and enthalpy of boiling. Best *et al.* (1997) applied a combination of Eqs. (6) and (10) to estimate ΔG°_{OA} using ΔG°_{AW} and $\log_{10} K_{OW}$.

TABLE 2. Summary of the different techniques used to obtain estimated K_{OA} values, including the K_{OA} and temperature ranges of the values reported in the database

Type of technique	Method	n	$\log_{10} K_{OA}$ range	Temperature range (°C)	References
QSPRs	Thermodynamic triangles	1297	−3.0–30.2	10–25	Abraham *et al.* (2001), Best *et al.* (1997), Finizio *et al.* (1997), Hiatt (1997); Kurz and Ballschmiter (1999), Meylan and Howard (2005), Odabasi *et al.* (2006a), Raevsky *et al.* (2006), Sepassi and Yalkowsky (2007), and Zhang *et al.* (2016)
	Regression models	5454	−0.4–29.1	−50–50	Abraham *et al.* (2005), Chen *et al.* (2003a; 2002a; 2003c; 2003b; 2002b; 2001; 2016), Cousins and Mackay (2000), Duffy and Jorgensen (2000), Ferreira (2001), Jiao *et al.* (2014), Jin *et al.* (2017), Kim *et al.* (2016), Li *et al.* (2006), Liu *et al.* (2013), Mathieu (2020), Nabi *et al.* (2014), Oliferenko *et al.* (2004), Papa *et al.* (2009), Puzyn and Falandysz (2005), Vikas and Chayawan (2015), Wang *et al.* (2008), Xu *et al.* (2007), Yuan *et al.* (2016), Zeng *et al.* (2013), Zhang *et al.* (2016), and Zhao *et al.* (2005)
	UPPER	182	1.2–15.6	25	Lian and Yalkowsky (2014) and Yalkowsky *et al.* (1994b)
	UNIFAC	73	0.4–2.4	25	Dallas (1995)
	Machine learning	22	7.4–12.2	25	Jiao *et al.* (2014)
Solvation models		3719	−1.2–28.4	−5–40	Best *et al.* (1997), Dallas (1995), Fu *et al.* (2016), Giesen *et al.* (1997), Li *et al.* (1999; 2020), Nedyalkova *et al.* (2019), Parnis *et al.* (2015), Zhang *et al.* (2016), Zhu *et al.* (1998)

Many works report K_{OA} values calculated using thermodynamic triangles or estimated using EPISuite^{TM} [e.g., Alarie *et al.* (1995), Sühring *et al.* (2016), Tamaru *et al.* (2019), and Xu *et al.* (2014)]. We have elected to not include all these K_{OA} values. When we did include K_{OA} values obtained through thermodynamic triangles in the database, we also report the original source of the two property values in the property table (see Sec. 4.2.5).

3.1.2. Regression models

Numerous regression models for predicting K_{OA} exist, most frequently restricted in applicability to a specific set of closely related compounds, such as the polychlorinated biphenyls (PCBs) and naphthalenes (PCNs) or the polybrominated diphenyl ethers (PBDEs). The models differ based on the compound group, the type of regression, and the source and type of chemical descriptors. The statistical techniques applied include ordinary or MLRs, partial least-squares models, and principal component regression models. Some models also incorporate temperature into the regression analysis (Chen *et al.*, 2003c; 2003b; 2002b; Jin *et al.*, 2017; and Li *et al.*, 2006). Tables 2 and 3 include a list of the K_{OA} models whose predictions are included in the database and the parameterization as described in this paper.

3.1.3. UPPER

The Unified Physical Property Estimation Relationship (UPPER) model by Yalkowsky *et al.* (1994a) uses the thermodynamic triangle between K_{OA}, P_L, and S_O [Eq. (9)]. Molecular descriptors are obtained from the structure of a chemical using additive-group contribution estimations or the geometry of the structure (Lian and Yalkowsky, 2014). The descriptors are then used to derive basic physical–chemical properties (referred to as component properties, including melting and boiling points), which allow for the calculation of K_{OA}, K_{AW}, and K_{OW} (Yalkowsky *et al.*, 1994a).

3.1.4. UNIFAC

The UNIFAC model estimates γ_O^{∞} with an additive fragment-based approach with group-interaction parameters (Fredenslund *et al.*, 1975). It also considers the volume, surface area, and the number of different groups present in the solute (Fredenslund *et al.*, 1975). Dallas (1995) used UNIFAC to estimate K_{OA} and compare it to direct measurements and the MOSCED model (see Sec. 3.2). This author also compared the performance of the UNIFAC model with an infinite-dilution activity based UNIFAC model, which uses calculated interaction parameters using activity coefficients at infinite dilution, and a modified

TABLE 3. A list of all the regression models whose K_{OA} predictions are included in the database. MLR: stepwise multiple linear regression models; OLS: ordinary least squares; PCR: principal component regression; PLS: partial least squares; SLR: single linear regression; and MC: Monte Carlo. Note that some of these papers referenced utilize existing models with new descriptors to obtain novel K_{OA} values

Compound class	Regression method	Descriptors	References
Methyl and alkyl substituted naphthalenes	MLR	Abraham descriptors	Abraham *et al.* (2005)
Methyl and alkyl substituted naphthalenes	MLR[a]	Abraham descriptors	Abraham *et al.* (2005)
PCDD/Fs	PLS	MOPAC descriptors	Chen *et al.* (2001)
PCBs	PLS	MOPAC descriptors	Chen *et al.* (2002a)
PCDD/Fs	PLS	MOPAC descriptors	Chen *et al.* (2002b)
PCNs, CBz	PLS	MOPAC descriptors	Chen *et al.* (2003a)
PCBs	PLS	MOPAC descriptors, theoretical descriptors (CS ChemOffice)	Chen *et al.* (2003b)
PBDEs	PLS	MOPAC descriptors, theoretical descriptors (CS ChemOffice)	Chen *et al.* (2003c)
PCBs	PLS	CoMFA	Chen *et al.* (2016)
PCBs	PLS	CoMSIA	Chen *et al.* (2016)
Phthalate esters	SLR	LeBas molar volume	Cousins and Mackay (2000)
Simple diverse compounds	MC and MLR	Total solvent-accessible surface area, solute–solvent Coulomb energy, hydrophobic SASA, number of solute as donor hydrogen bonds	Duffy and Jorgensen (2000)
PAHs	PLS	Electronic descriptors (MOPAC), topological descriptors [see Ferreira (2001) for equations], geometric descriptors [Sanders and Wise Database, see Ferreira (2001) for equations]	Ferreira (2001)
PBDEs	MLR	Molecular distance-edge vector indexes	Jiao *et al.* (2014)
POPs, other hydrocarbons	MLR	Abraham descriptors	Jin *et al.* (2017)
PCDDs	SLR	Molecular descriptors[b]	Kim *et al.* (2016)
POPs	MLR	Fragment constant approach	Li *et al.* (2006)
PBDEs	PLS	CoMFA	Liu *et al.* (2013)
PBDEs	PLS	CoMSIA	Liu *et al.* (2013)
Diverse compounds	MLR	Additive approach using geometric fragments[c]	Mathieu (2020)
Nonpolar organic compounds	MLR	Abraham descriptors	Nabi *et al.* (2014)
Nonpolar organic compounds	MLR	CODESSA PRO QSAR software and hydrogen bonding descriptor	Nabi *et al.* (2014)
PBDEs, other hydrocarbons	OLS	DRAGON descriptors	Papa *et al.* (2009)
PCNs	PCR	Quantum-chemical descriptors (GAUSSIAN 03), topological descriptors (DRAGON)	Puzyn and Falandysz (2005)
PCDD/Fs	SLR	Quantum-chemical descriptors[b]	Vikas and Chayawan (2015)
PBDEs	MLR	Quantum-chemical based structural parameters (Gaussian98)	Wang *et al.* (2008)
PBDEs	MLR	Electrostatic potential indices (MOPAC and Gaussian98), physicochemical properties (TSAR)	Xu *et al.* (2007)
PCBs	MLR	DRAGON descriptors	Yuan *et al.* (2016)
PCBs	PLS	HQSAR descriptors	Yuan *et al.* (2016)
PCDDs	MLR	Quantum-chemical based structural parameters (Gaussian98)	Zeng *et al.* (2013)
Pesticides	MLR	Abraham descriptors[d]	Zhang *et al.* (2016)
CBz	MLR	Molecular connectivity indexes	Zhao *et al.* (2005)
PAHs	MLR	Molecular connectivity indexes	Zhao *et al.* (2005)
PBDES	MLR	Molecular connectivity indexes	Zhao *et al.* (2005)
PCDD/Fs	MLR	Molecular connectivity indexes	Zhao *et al.* (2005)
PCNs	MLR	Molecular connectivity indexes	Zhao *et al.* (2005)

[a]For wet-octanol.
[b]Multiple models using different descriptors are presented in the papers and included in the database.
[c]Coefficients for each fragment (characteristic temperature) are obtained via MLR.
[d]Uses the ABSOLV model from ACD/Labs.

UNIFAC model that combines the original and the infinite-dilution activity based UNIFAC models. A summary of publicly available group-interaction parameters can be obtained from the UNIFAC Consortium webpage (http://unifac.ddbst.de/unifac_.html). Note that within the database, we include estimates that directly report K_{OA} or include a P_L for the calculation of K_{OA}. Papers that only report a UNIFAC-estimated γ_o^∞ are not included [e.g., Castells *et al.* (1999), Eikens (1993), and Li *et al.* (1995)].

3.1.5. Machine learning

While machine learning algorithms resemble regression models in that they use descriptors to predict K_{OA}, they differ in the approach to correlating the different variables. Jiao *et al.* (2014) created an artificial neural network model that uses molecular distance-edge vector index descriptors to predict K_{OA}. The model is designed to have the smallest RMSE for the validation set (Jiao *et al.* 2014).

The OPERA model (Mansouri *et al.*, 2018; Mansouri and Williams, 2017) is also a QSAR model developed using machine learning. OPERA uses the *k*-nearest neighbor approach and PaDEL descriptors for the number of hydrogen bond donor and the hexadecane-air partition ratio to estimate K_{OA}. While estimates from OPERA are not included in the database, these values are easily obtained from the CompTox Dashboard (Williams *et al.*, 2017) or the model can be downloaded from GitHub (https://github.com/kmansouri/OPERA).

3.2. Solvation models

Solvation models estimate the ΔG_i° of a chemical in a solvent *i*. The difference of ΔG_i° in octanol and the gas phase can be used to estimate ΔG_{OA}°, which, in turn, can be used to estimate K_{OA} (Nedyalkova *et al.*, 2019). Such models have been applied to estimate K_{OA} of a wide range of chemicals, and numerous variations of models for estimating ΔG_{OA}° exist in the literature. The information included in the database is limited to models that have been specifically designed to estimate ΔG_{OA}° and to predictions made during the comparison and assessment of these solvation estimation techniques. A subset of universal solvation models that estimate ΔG° for various air–solvent interactions are also considered. Specifically, this includes estimates from MOSCED (Modified Separation of Cohesive Energy Density) (Thomas and Eckert, 1984) and various universal solvation models [e.g., Best *et al.* (1997)].

The MOSCED model estimates ΔG_i° in a solvent as the difference between the cohesive energy density of the pure phase and the solution (Thomas and Eckert, 1984). The SM8AD and SMD models are universal solvation models that solve for the electrostatic contribution using either the generalized Born approximation with asymmetric de-screening (SM8AD) (Marenich *et al.*, 2009a) or the nonhomogeneous Poisson equation (SMD) (Marenich *et al.*, 2009b). These models can be parameterized using different density functionals, which can produce slightly different results (Nedyalkova *et al.*, 2019). Multiple variations of these solvation models for multiple solvents exist, and we have included a selection of estimates, such as Best *et al.* (1997), Duffy and Jorgensen (2000), Giesen *et al.* (1997), Li *et al.* (1999), and Zhu *et al.* (1998). While there are very likely far more universal solvation models for ΔG_{OA}° in the literature, we have included only selected estimates in the database because these models often merely improve upon previous iterations of the SM-AD and SMD models and predict the ΔG_{OA}° for sets of chemicals that also have experimental ΔG_{OA}° values.

The COnductor-like Screening Model for Realistic Solvents (COSMO-RS) software suite can also be used to estimate K_{OA} for chemicals [e.g., Parnis *et al.* (2015)]. COSMO-RS applies quantum chemical density functional theory and statistical thermodynamics to derive ΔG° values (Klamt *et al.*, 2009). Endo and Hammer (2020) introduced a fragment contribution model for extrapolating COSMO-RS predicted K_{OA} for short-chain chlorinated paraffins, which reduces calculation times.

TABLE 4. MLR models for predicting K_{OA}, which have not been included in the database because no K_{OA} estimates are published directly

Chemical specificity	Regression method	Descriptor	References
POPs	PLS	Quantum chemical descriptors	Chen *et al.* (2004)
Diverse compounds	PLS	Quantum chemical descriptors (DRAGON)	Fu *et al.* (2016)
Diverse compounds	PLS	Atom-centered fragments (DRAGON)	Fu *et al.* (2016)
Chlorinated compounds	MLR	Molecular polarizabilities and multipole moments (GAUSSIAN 98)	Staikova *et al.* (2004)
PCNs	MLR	Abraham descriptors	Abraham and Al-Hussaini (2001)
N-nitrosodialkylamines	MLR	Abraham descriptors	Abraham and Al-Hussaini (2002)
Diverse compounds	MLR	Abraham descriptors	Abraham and Acree (2008)
Diverse compounds	MLR	Abraham descriptors	Abraham *et al.* (2008)
Diverse compounds	MLR	Abraham descriptors	Endo and Goss (2014)
Diverse compounds	MLR	General treatment of solute–solvent interactions (GSSI) descriptors	Deanda *et al.* (2004)
PCNs	PLS	MOPAC and 3D-HoVAIF descriptors	Li *et al.* (2012)
Organophosphorus compounds	MLR	Abraham descriptors	Abraham and Acree (2013)

3.3. Other models for estimating K_{OA}

Another tool for estimating K_{OA} is SPARC Performs Automated Reasoning in Chemistry's online physicochemical calculator (SPARC) (available at http://archemcalc.com/). The details on how exactly SPARC works are not widely available. However, it is noted that linear free energy relationships are used to estimate thermodynamic properties such as K_{OA} (Hilal *et al.*, 2003). While SPARC has been applied repeatedly to estimate K_{OA} (Zhang *et al.*, 2016), the calculated K_{OA} values are not often reported [e.g., Stenzel *et al.* (2014) and Wang *et al.* (2012)]. We only include K_{OA} estimates from SPARC in the database if they are compared to experimental values or other estimates; thus, K_{OA} values reported in papers such as Weschler and Nazaroff (2010) have not been included.

Some other publications on K_{OA} estimation models, including various MLR models such as poly-parameter linear free-energy relationships (ppLFERs), COSMO*therm* (Klamt, 2018; 2011), and OPERA (Mansouri *et al.*, 2018), do not always report the estimated K_{OA} values. Thus, K_{OA} estimates made with these approaches are not included in the database. In addition, there are published MLR models for predicting K_{OA} that do not report estimated K_{OA} values and thus are not included in the database; a summary of these models is included in Table 4.

Some models have been designed to estimate the temperature dependence of $\log_{10} K_{OA}$ for a series of compounds. For example, the model by Yang *et al.* (2018) estimates the temperature dependence of K_{OA} for PBDEs. Mintz *et al.* (2008; 2007) published two ppLFERs using Abraham descriptors to estimate ΔH°_{OA} of a wide range of chemicals.

4. K_{OA} Data

4.1. Data collection

This database includes all measured or estimated K_{OA} values that we could locate in the literature using the Web of Science using variations of the keywords: *Octanol–air partition coefficient* (K_{OA}), *octanol–gas partition coefficient*, *Ostwald coefficient octanol*, and *Gibbs free energy octanol*. References were also found by looking up citations included in the identified papers. A total of 112 literature sources were found to contain K_{OA} data. Forty-seven sources included estimated K_{OA} values, while 70 contained measured values. The database incorporates 209 K_{OA} values from three dissertation theses (Cheong, 1989; Dallas, 1995; and Özcan, 2013). While a large portion of the work by Dallas (1995) was published in Abraham *et al.* (2001) and Dallas and Carr (1992), a portion of K_{OA} estimates from this thesis are not available in the peer-reviewed literature. To the best of our knowledge, K_{OA} data from Cheong (1989) and Özcan (2013) have not been published in the peer-reviewed literature. The search was limited to publications written in English, although articles containing $\log_{10} K_{OA}$ estimates have also been published in other languages [e.g., Zhang *et al.* (2005) and Zou *et al.* (2005)].

We have included the error of a measurement or estimation in the database. We have also noted where the K_{OA} reported is for a mixture of isomers or the chemical structure is ambiguous [e.g., Harner and Bidleman (1998), Kömp and McLachlan (1997), and Vuong *et al.* (2020)]. In some instances where a single paper has reported more than one K_{OA} using different techniques, we note which technique or value was recommended by the authors [e.g., Su *et al.* (2002)].

4.2. Database structure

The database is provided in a Microsoft Excel workbook and as an R package. The data are stored in seven distinct tables (Fig. 3) to allow users to sort and filter the data based on various criteria, including author, publication year, and measurement or estimation technique.

The Chemical Table provides information regarding the name, CAS number, SMILES notation, and other chemical identifiers for each solute. Each unique chemical is associated with a chemical identification number within the database (chemID). Similarly, each unique literature source and author are assigned a unique identifier in the Reference Table (refID) and Author Table (auID). The Author-Reference Table is used to connect the information presented in both. Each method for predicting or estimating K_{OA} within a paper is also assigned a unique identifier (methID). The Property Table contains the P_L, γ_{oct}, K_{AW}, K_{OW}, and ΔG° values originally reported in the paper in SI units (with the exception of ΔG°, which is in kJ mol^{-1}) and used to calculate the K_{OA}; each value is assigned a propID. Finally, the K_{OA} values are reported in the K_{OA} Table, with each datapoint uniquely associated with a dataID.

4.2.1. Chemical table

The QSAR-ready SMILES notation for the 1643 compounds with literature data was taken from EPA's CompTox Dashboard (Williams *et al.*, 2017) or PubChem (Kim *et al.*, 2017) or, if none were available, created using ChemDraw. CAS numbers and names of chemicals were verified using both SciFinder and the CompTox Dashboard. Canonical SMILES for compounds were produced using Open Babel (version 3.00) (O'Boyle *et al.*, 2011). We also include the IUPAC name, common name, common acronym, and alternative names and acronyms for each chemical. The list of names for each compound is not exhaustive, and we recommend searching for chemicals using their CAS number. We also group chemicals into over 50 broad categories, including PCBs, PBDEs, PCNs, amines, ketones, and so on. This categorization of chemicals is also nonexhaustive as many chemicals may fall into more than one group. Within the database, each chemical is assigned a unique identifier, a chemID. In some instances, the K_{OA} of a mixture of two or more chemicals is also reported, these mixtures are also given a unique chemID, and the CAS number and the identifying information for all chemicals in the mixture are included.

4.2.2. K_{OA} table

K_{OA} data are stored in the K_{OA} Table. Each K_{OA} value is assigned a unique identifier (dataID), which is associated with a specific chemical (chemID) and method (methID). For each K_{OA} value, we also include the temperature of the measurement, any errors reported for the measurement, and comments or notes for the datapoint. The comments indicate if the K_{OA} reported is for an isotopically labeled species or if any typo corrections and assumptions were made during the data curation process of the original work.

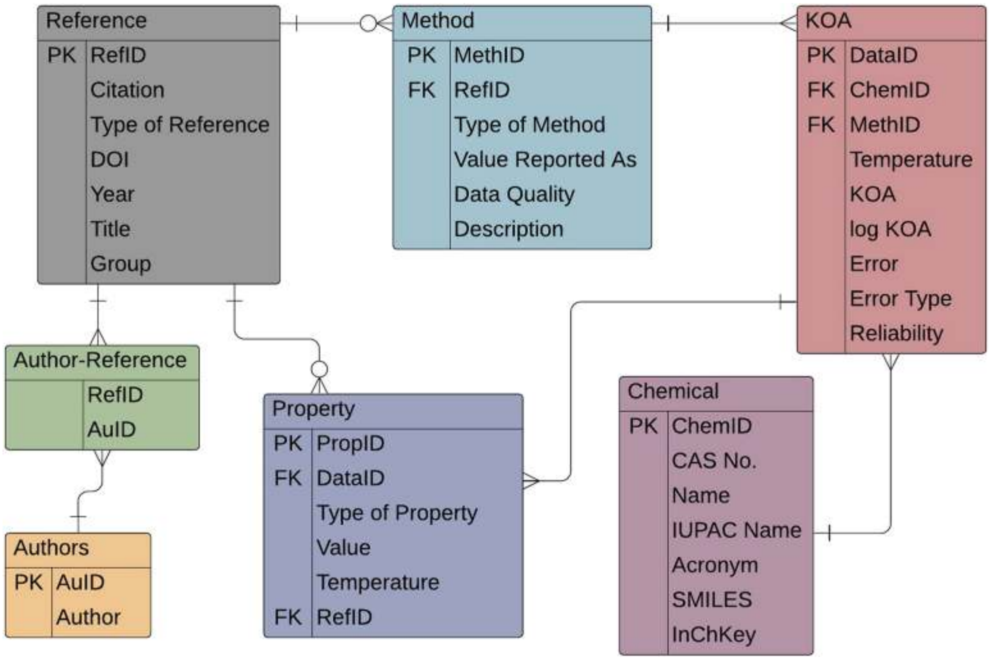

FIG. 3. A relational schematic representation of the K_{OA} database. PK denotes a primary key, which is unique to a specific table. FK denotes a foreign key, which indicates how the data in the different tables are connected.

4.2.3. Methods and reference table

Each reference is stored in the Reference Table and assigned a unique identifier (refID). Some references may report or compare the results of different K_{OA} measurement or experimental techniques; therefore, a single reference can be associated with multiple experimental and estimation techniques. Each technique from each reference is also assigned a unique identifier (methID). Different measurement and estimation techniques have been employed and published at different times over the past few decades, which is shown in Fig. SI 7 in the supplementary material.

4.2.4. Property table

In Sec. 1.1, we discussed the different ways $\log_{10} K_{OA}$ has been reported in the literature. The Property Table (dark blue table, Fig. 3) includes the data originally reported in the literature in standardized units, except ΔG°, which is reported in units of kJ mol^{-1}. This includes converting all reported k_H values to K_{AW} for convenience. Each property value within the database is associated with exactly one K_{OA} datapoint in the main K_{OA} Table; however, a single K_{OA} datapoint may be associated with more than one property value. Each property datapoint is associated with a chemical (chemID), method (methID), reference (refID), and K_{OA} value (dataID). There are 2228 dataIDs that are associated with 3723 propIDs. Figure SI 4 shows the distributions of the different property data included in the database.

4.3. Quality of the reporting

Each technique and method (i.e., methID) for determining and reporting K_{OA} values was assigned a score based on whether

(i) the method is an estimation or empirical technique,
(ii) the description of the used methodology is sufficiently detailed,
(iii) some analysis of the methods is provided (including, e.g., their possible limitations and scope), and
(iv) an error of the K_{OA} value is reported and/or whether an external validation of the K_{OA} value was performed.

Each factor is weighted equally, and the papers are thus scored from 0 to 4. The point assigned for each factor is binary, and thus, there are no half points allocated. These points are only ascribed to method, description, analysis, and error of the reported K_{OA} value. For example, a method from a paper about empirical measurements of K_{OA}, providing a detailed description and analysis of the methodology and the error of the prediction, will have a score of 4, whereas a thermodynamic triangle method without any additional details or analysis will have a score of 1. Based on this categorization, a total of 36 methods scored 4, 81 methods scored 3, 32 methods scored 2, and 14 methods scored 1. Note that we define each method as having a unique identifier (methID). Figure SI 2 shows the distribution of the scores across the $\log_{10} K_{OA}$ range for experimental and estimated data.

4.4. K_{OA} data

The database contains 13 264 K_{OA} values for 1643 different chemicals between −50 and 110 °C. Of these, 2517 values (19%) are experimentally derived and 10 747 values (81%) are estimated (Fig. 4). Notably, the data are bimodally distributed with respect to $\log_{10} K_{OA}$, with one maximum between $\log_{10} K_{OA}$ 2 and 4 and a

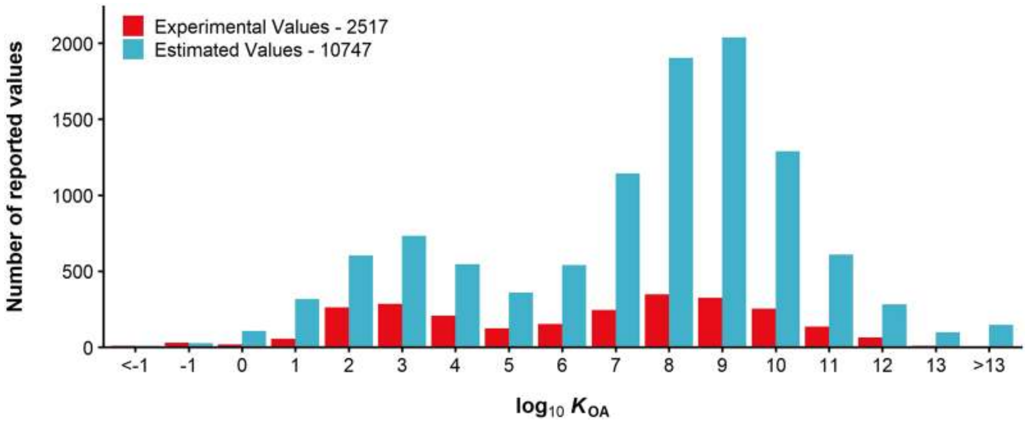

FIG. 4. Distribution of all experimental and estimated K_{OA} values included in the database.

second between $\log_{10} K_{OA}$ 6 and 11. If we consider only measurements or estimates made at 25 °C, the peaks become even more pronounced (Fig. SI 1). These peaks are a result of the difference in the applicability range of the different measurement techniques. Many estimation techniques require a set of K_{OA} data to develop and train new models, so the distribution of estimated K_{OA} values follows a similar pattern.

4.5. Measured K_{OA} values

There are 2517 measured K_{OA} values in the database for 704 chemicals. Of these, 1524 are directly measured values, while 993 are obtained by indirect measurements using chromatographic retention time techniques. The highest and lowest determined $\log_{10} K_{OA}$ values are −1.8 and +14 for helium (CAS No. 7440-59-7) and trichloro-benzo[a]pyrene (CAS No. 97303-27-0), respectively. Most of the reported values (52%) are for $\log_{10} K_{OA}$ values between 6 and 11, followed by measurements between 2 and 5 (30%). Few measurements have been reported for chemicals with a $\log_{10} K_{OA}$ less than 2 (4%) or greater than 11 (8%). There is also a drop in the number of measurements between $\log_{10} K_{OA}$ 5–6 (4.92%). Most $\log_{10} K_{OA}$ values less than 4 are measured directly using static techniques, while dynamic or indirect techniques were used to measure $\log_{10} K_{OA}$ values greater than 6 [Fig. 6, Panel (a)]. Approximately, a quarter (26.2%) of measurements in the database were obtained using static techniques, a third (34.2%) using dynamic techniques, and 39.4% using indirect techniques. Figure 5 displays in more detail the K_{OA} range in which different static and dynamic techniques have been applied.

There are 924 K_{OA} values (37%) for 573 chemicals at 25 °C, and most measurements (51%) are made within the 20–30 °C range. There are relatively more measurements made at high temperatures (>30 °C) when $\log_{10} K_{OA}$ is less than 3, presumably to extend the

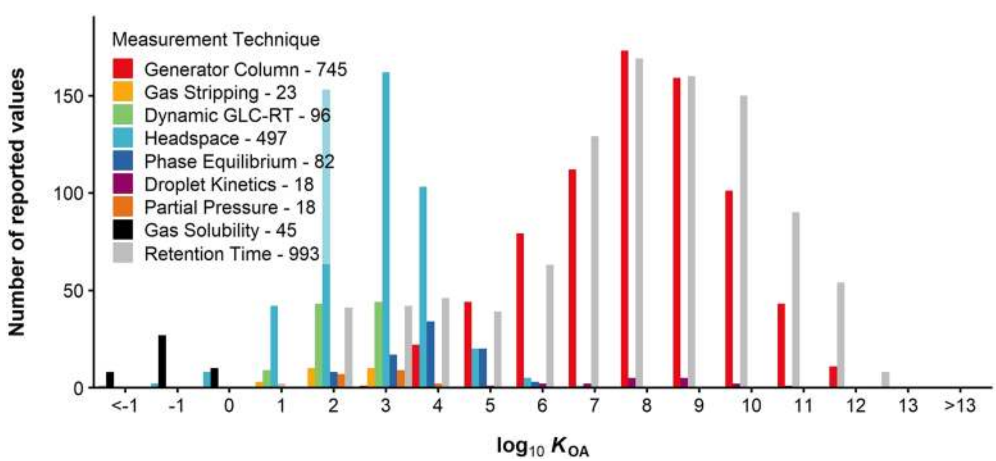

FIG. 5. Distribution of different methods used across a $\log_{10} K_{OA}$ range of < −1 to > 13. The generator column, gas stripping, and dynamic GLC-RT are dynamic techniques. Headspace, phase equilibrium, droplet kinetics, partial pressure, and gas solubility methods are static techniques.

TABLE 5. A summary of all papers and techniques reporting experimental K_{OA} values that are included in the database, including the type of methodology and the $\log_{10} K_{OA}$ and temperature ranges for each method

References	Method	Technique	*n*	$\log_{10} K_{OA}$ range	Temperature range (°C)	Compound groups
Wilcock *et al.* 1978	MA	Gas solubility	26	−1.79–0.24	9.3–40.49	Gases
Bo *et al.* 1993	BN-B	Gas solubility	9	−1.57–0.24	25	Gases
Abraham *et al.* 2001	HS and GC	Headspace	81	−1.29–5.36	25	Hydrocarbons, halogenated
Boyer and Bircher 1960	Vgas	Gas solubility	5	−0.99–0.42	25	Gases
Taheri *et al.* 1993	HS Vac	Headspace	6	−0.43–4.36	37	Alkanes
Fang *et al.* 1997b	HS Vac	Headspace	6	−0.31–1.78	37	Haloalkanes
Pollack *et al.* 1984	PM	Gas solubility	5	0.27–0.45	10–50	Xenon
Hiatt 1997	VD/GC/MS	Headspace	113	0.48–5.57	25	Hydrocarbons, PAHs, CBz, halogenated, amines, labeled
Taheri *et al.* 1991	HS Vac	Headspace	7	1.14–2.5	37	Haloalkanes
Ionescu *et al.* 1994	HS Vac	Headspace	2	1.52–1.73	37	Halogenated compounds
Ionescu *et al.* 1994	HS Vac	Headspace	2	1.56–1.78	37	Halogenated compounds
Lei *et al.* 2019	VPHS	Headspace	78	1.58–4.4	25–110	Various hydrocarbons
Gruber *et al.* 1997	GLC-RT	GLC-RT	96	1.63–3.92	20.29–50.28	Alkanes, alkenes, cyclic, arenes, alcohols
Fukuchi *et al.* 2001	GS	Gas stripping	4	1.65–2.12	10–40	Haloethers
Eger *et al.* 2001	HS Vac	Headspace	4	1.75–2.51	37	Haloalkanes, haloarenes
Dallas 1995	HS and GC	Headspace	75	1.75–5.36	25	Simple hydrocarbons
Bhatia and Sandler 1995	GLC-RT	Retention time	32	1.91–3.6	25–50	Haloalkanes, alkanes
Tse and Sandler 1994	GLC-RT	Retention time	15	1.95–3.6	25	Alkanes, Cl and Br alkyl halides
Cheong 1989	HS and GC	Headspace	11	2.02–3.9	25	Alkanes
Eger *et al.* 1997	HS Vac	Headspace	3	2.13–2.14	37	Isoflurane
Fukuchi *et al.* 1999	GS	Gas stripping	9	2.16–3.1	10–30	Ether
Berti *et al.* 1986	PP	Vapor pressure	8	2.16–3.66	25	Simple hydrocarbons
Fang *et al.* 1996	HS Vac	Headspace	20	2.16–3.87	37	Haloarenes, arenes, cyclic
Fang *et al.* 1997a	HS Vac	Headspace	5	2.21–6.01	37	Alcohols
Park *et al.* 1987	HS and GC	Headspace	6	2.53–3.42	25	Simple hydrocarbons
Batterman *et al.* 2002	HS and GC	Headspace	4	2.55–3.97	37	Halogenated alkanes
Hussam and Carr 1985	HS and GC	Headspace	2	2.59–3.3	25.01	Nitroxy, arene
Rohrschneider 1973	HS	Headspace	6	2.61–3.37	25	Nitromethane, toluene
Su *et al.* 2002	MR-SC-GC-RT	Retention time	230	2.65–12.39	10–50	PCNs, CBz
Xu and Kropscott 2014	3P-Eqbm	Phase equilibrium	26	2.69–5.68	4.2–35.2	Organosiloxanes
Xu and Kropscott 2013	2P-Eqbm	Phase equilibrium	49	2.71–6.85	−5–40.2	Organosiloxanes
Cabani *et al.* 1991	PP	Vapor pressure	10	2.75–4.07	25	Simple hydrocarbons
Su *et al.* 2002	MR-GC-RT	Retention time	110	2.86–11.31	10–50	PCNs, CBz
Dallas and Carr 1992	HS and GC	Headspace	11	2.87–5.18	25	Alcohols

TABLE 5. (*Continued*)

References	Method	Technique	n	$\log_{10} K_{OA}$ range	Temperature range (°C)	Compound groups
Roberts 2005	Bubbler	Gas stripping	5	2.92–3.39	0–25	Peroxyacetyl nitrate
Su *et al.* 2002	MR-GC-RT	Retention time	78	2.99–11.28	10–50	PCNs, CBz
Eger *et al.* 1999	HS Vac	Headspace	19	3–5.99	37	Alcohols, FTOHs
Treves *et al.* 2001	SPME	Headspace	9	3.03–7.88	25	Alkyl dinitrates, Alkyl nitrates, chlorobenzenes, PAHs
Eger *et al.* 1999	HS Vac	Headspace	19	3.06–6.01	37	Alcohols, FTOHs
Lei *et al.* 2004	SR-GC-RT	Retention time	12	3.19–7.09	25	Fluorinated
Leng *et al.* 2015	Bubbler	Gas stripping	5	3.45–3.85	5–25	Triethylamine
Hiatt 1998	VD/GC/MS	Headspace	8	3.68–4.28	25	Terpenes
Dreyer *et al.* 2009	FM	Generator column	52	3.99–6.95	5–40	FTAs, FOSA, FOSE
Thuens *et al.* 2008	FM	Generator column	37	4.1–6.79	5–40	FTOHs
Xu and Kropscott 2012	2P-Eqbm	Phase equilibrium	4	4.29–6.4	20.1–24.6	Organosiloxanes
Harner and Mackay 1995	FM	Generator column	60	4.36–11.83	−10–25	CBz, PCBs, DDT
Xu and Kropscott 2012	3P-Eqbm	Phase equilibrium	3	4.4–5.72	21.7–24.6	Organosiloxanes
Goss *et al.* 2006	FM	Generator column	11	4.8–6.72	0–25	FTOHs
Yaman *et al.* 2020	SR-GC-RT	Retention time	14	5.15–11.78	25	OPEs
Ha and Kwon 2010	droplet kinetics	Droplet kinetics	10	5.37–10.48	25	PAHs
Harner and Bidleman 1998	FM	Generator column	159	6.09–10.62	0–50	PAHs, PCNs
Zhang *et al.* 1999	MR-GC-RT	Retention time	208	6.09–13.36	0–20	PCBs
Odabasi *et al.* 2006a	SR-GC-RT	Retention time	14	6.34–12.59	25	PAHs
Özcan 2013	SR-GC-RT	Retention time	11	6.43–8.77	25	Musks
Kömp and McLachlan 1997	FM	Generator column	96	6.52–10.66	10–43	PCBs
Okeme *et al.* 2020	SR-GC-RT	Retention time	49	6.59–11.44	25	PCBs, musk, PAHs, DDTs, other hydrocarbons
Harner and Bidleman 1996	FM	Generator column	86	6.64–12.57	−10–30	PCBs
Wania *et al.* 2002	SR-GC-RT	Retention time	45	6.78–12.15	25	PBDEs, PCBs, PCNs
Wania *et al.* 2002	FM	Generator column	8	6.95–8.93	5–45	Alkanes
Pegoraro *et al.* 2015	SR-GC-RT	Retention time	8	7–11.18	25	Phthalates, cinnamate
Shoeib and Harner 2002b	FM	Generator column	112	7.38–11.38	5–45	OCPs
Harner *et al.* 2000	FM	Generator column	57	7.4–11.66	0–50	PCDD/Fs, PCB
Shoeib *et al.* 2004	FM	Generator column	12	7.44–8.8	0–25	PFAS
Wang *et al.* 2017	SR-GC-RT	Retention time	14	7.55–13.5	25	Organophosphates
Zhang *et al.* 2009	SR-GC-RT	Retention time	7	7.61–9.87	25	DDT, HCH
Odabasi *et al.* 2006b	SR-GC-RT	Retention time	2	7.68–8.03	25	PAH, carbozole
Yao *et al.* 2007	FM	Generator column	4	7.93–8.88	20	Pesticides
Vuong *et al.* 2020	SR-GC-RT	Retention time	34	8.06–13.98	25	PAHs
Shoeib and Harner 2002a	MR-GC-RT	Retention time	16	8.12–10.8	23	PCBs
Zhao *et al.* 2010	SR-GC-RT	Retention time	29	8.3–13.29	25	PBDEs
Chen *et al.* 2001	RTI	Retention time	29	8.36–12.05	25	PCDD/Fs
Odabasi and Cetin 2012	SR-GC-RT	Retention time	7	8.41–10.57	25	Cyclodienes
Zhao *et al.* 2009	SR-GC-RT	Retention time	12	8.5–12.7	10–25	FTOHs, PFASs
Harner and Shoeib 2002	FM	Generator column	51	8.52–12.64	15–45	PBDEs
Lee and Kwon 2016	droplet kinetics	Droplet kinetics	8	8.85–11.01	25	BFRs
Harner *et al.* 2000	RTI	Retention time	17	10.9–13	7	PCDD/Fs

applicability of static techniques to somewhat less volatile chemicals. More surprisingly, there are also relatively more measurements at cooler temperatures (<20 °C) when $\log_{10} K_{OA}$ is greater than 7 [Fig. 6, Panel (b)]. This is likely because many of those less volatile chemicals are environmental contaminants and the partitioning behavior at environmentally relevant temperatures is of primary interest. Measurements in the $\log_{10} K_{OA}$ range between 7 and 10 have been made at the most diverse range of temperatures.

The types of chemicals for which directly measured K_{OA} values have been reported are shown in Table 5. Chemicals with measured $\log_{10} K_{OA}$ values greater than 6 are generally persistent organic pollutants, including CBz, PCBs, PAHs, PCNs, and PBDEs

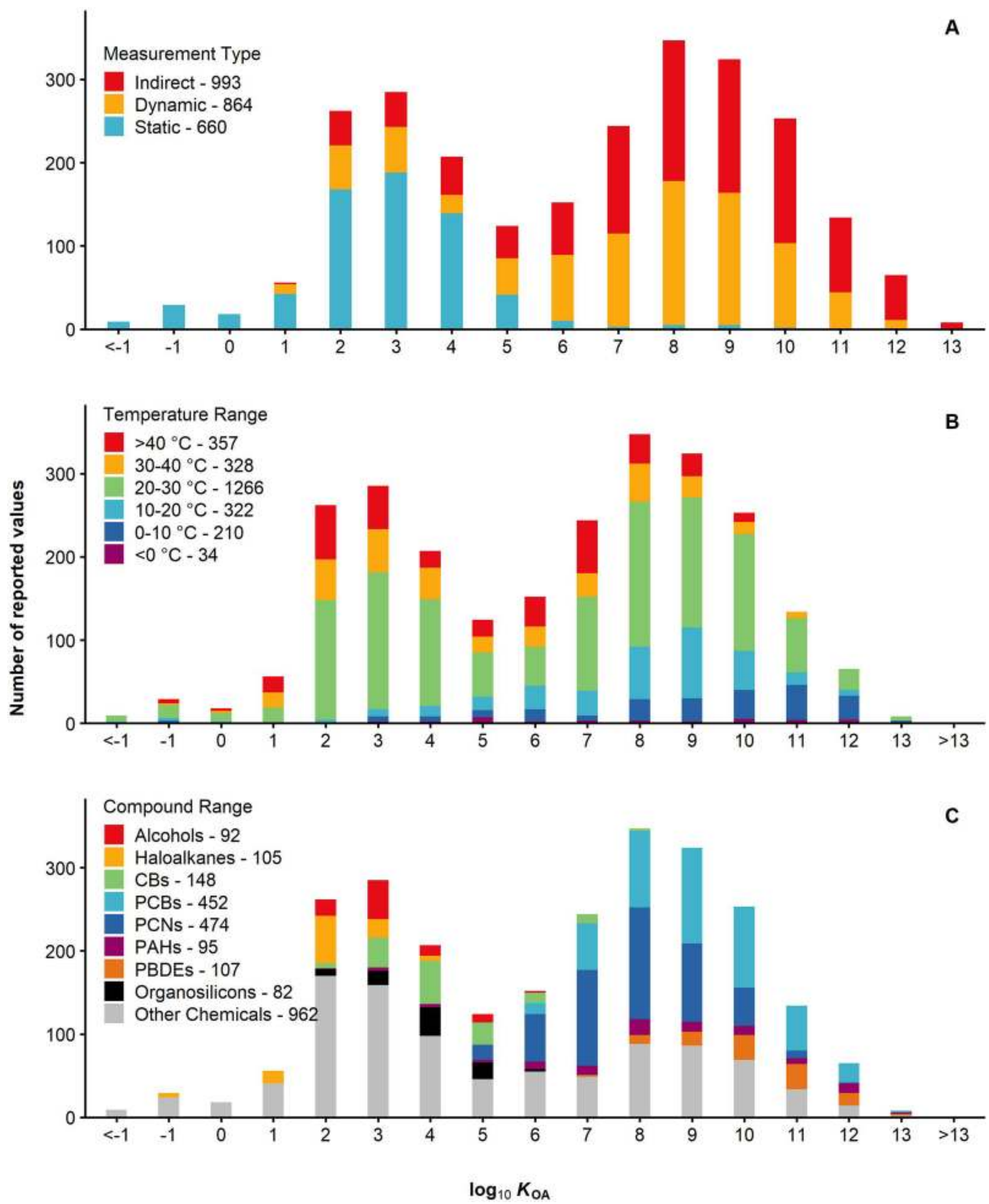

FIG. 6. Distribution of experimentally derived $\log_{10} K_{OA}$ values included in the database. Each panel shows the distribution based on the experimental technique used [Panel (a)], the temperature range of the reported value [Panel (b)], and common classes of chemicals with measured K_{OA} values [Panel (c)].

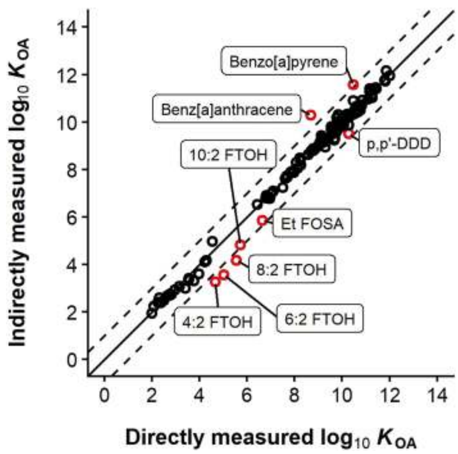

FIG. 7. Plot of directly versus indirectly measured K_{OA} for compounds for which values from both techniques exist. The solid line indicates a one-to-one relationship, while dashed lines represent ±1.

[Fig. 6, Panel (c)]. There is greater diversity among the chemicals with low measured $\log_{10} K_{OA}$ values, including simple hydrocarbons such as alkanes, alkenes, cyclic hydrocarbons, haloalkanes, alcohols, and organosilicons. Measurements of K_{OA} for small, volatile molecules are often motivated by explorations of basic partitioning behavior (Abraham *et al.*, 2001) or methodological issues (e.g., Lei *et al.*, 2019). At the very low $\log_{10} K_{OA}$ range (<1) are typically short chain alkanes, noble gases, and inorganic gases [e.g., xenon (CAS No. 7440-63-3) and carbon monoxide (CAS No. 630-08-0)].

4.6. Reliability of K_{OA} measurements

A subset of experimental $\log_{10} K_{OA}$ data was assessed to be unreliable. These measurements were made for polar compounds using a gas chromatography retention time (GC-RT) technique. Figure 7 compares K_{OA} values obtained using GC-RT methods against directly measured values, if they are available. While there is generally very good agreement between the reported values, some notable exceptions become apparent. K_{OA} values for a series of fluorotelomer alcohols (FTOHs) measured with the GC-RT technique are much lower than those measured using the generator column technique. We suspect that the GC-RT measurements are erroneous due to the high polarity of these compounds and their ability to undergo hydrogen bonding. These compounds would be expected to interact much more strongly with octanol than with the nonpolar GC column used, particularly relative to hexachlorobenzene (CAS No. 118-74-1), the reference compound used in the study (Lei *et al.* 2004). Thus, when measured with GC-RT, $\log_{10} K_{OA}$ for such chemicals tend to be too low.

Large discrepancies are also apparent for benz[a]anthracene (CAS No. 56-55-3) and benzo[a]pyrene (CAS No. 50-32-8), where K_{OA} values from the GC-RT techniques (Odabasi *et al.* 2006a) are much higher compared to those obtained with the droplet kinetics technique (Ha and Kwon 2010). In Fig. SI 3, we compare the measurements made using the droplet kinetics technique against other experimental measurements for the same compounds. The K_{OA} for benz[a]anthracene by Ha and Kwon (2010) is almost an order of magnitude smaller than most other measured and estimated values for this compound. On the other hand, the value obtained by GC-RT is within 0.5 $\log_{10}$ units of estimates using solvation models (Fu *et al.* 2016), the UPPER model (Lian and Yalkowsky 2014), and thermodynamic triangles (Sepassi and Yalkowsky 2007). The $\log_{10} K_{OA}$ for benzo[a]pyrene by Ha and Kwon (2010) is also lower than almost all other reported values. The GC-RT derived $\log_{10} K_{OA}$ for both PAHs is in excellent agreement with the final adjusted value derived by Ma *et al.* (2010). In addition, as these PAHs are relatively

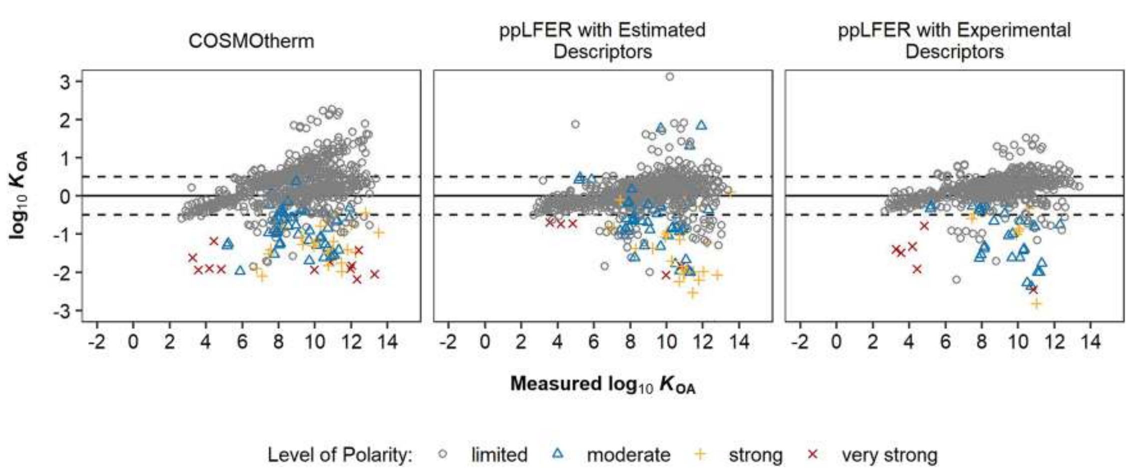

FIG. 8. Comparing the indirectly measured K_{OA} values against estimates made using ppLFER equations (Endo and Goss 2014) with estimated and experimental solute descriptors and COSMOtherm. Gray circles indicate limited polarity ($aA + bB < 0.5$), blue triangles indicate moderate polarity ($0.5 < aA + bB < 1$), yellow + indicate strong polarity ($1 < aA + bB < 2$), and red Xs indicate very strong polarity ($aA + bB > 2$). The dashed lines indicate a residual of $\pm 0.5 \log_{10}$ units between the experimental and estimated value.

non-polar, the GC-RT technique should be applicable and, in any case, not lead to K_{OA} values that are too high. We therefore suspect that in this case, the values reported by Ha and Kwon (2010) are more likely to be erroneous than the GC-RT values.

There are many more GC-RT-derived K_{OA} values without complementary directly measured values. To identify other potentially flawed values, we compared the GC-RT measured value with predictions made by three different prediction models. Figure 8 displays the residuals between predicted and GC-RT measured values, whereby chemicals are color-coded by the strengths of their H-bonding with octanol. The latter is quantified as $aA + bB$, where A and B are the Abraham solute descriptors for hydrogen bonding acidity and basicity of the solute and a and b are the respective system constants from the poly-parameter linear free energy equation for $\log_{10} K_{OA}$ by Endo and Goss (2014). Experimental solute descriptors were obtained using the UFZ-LSER Database (Ulrich *et al.* 2017); if experimental solute descriptors were unavailable, estimated solute descriptors were obtained using the IFSQSAR model developed by Brown and available on GitHub (https://github.com/tnbrowncontam/ifsqsar) (Brown 2014; Brown *et al.* 2012).

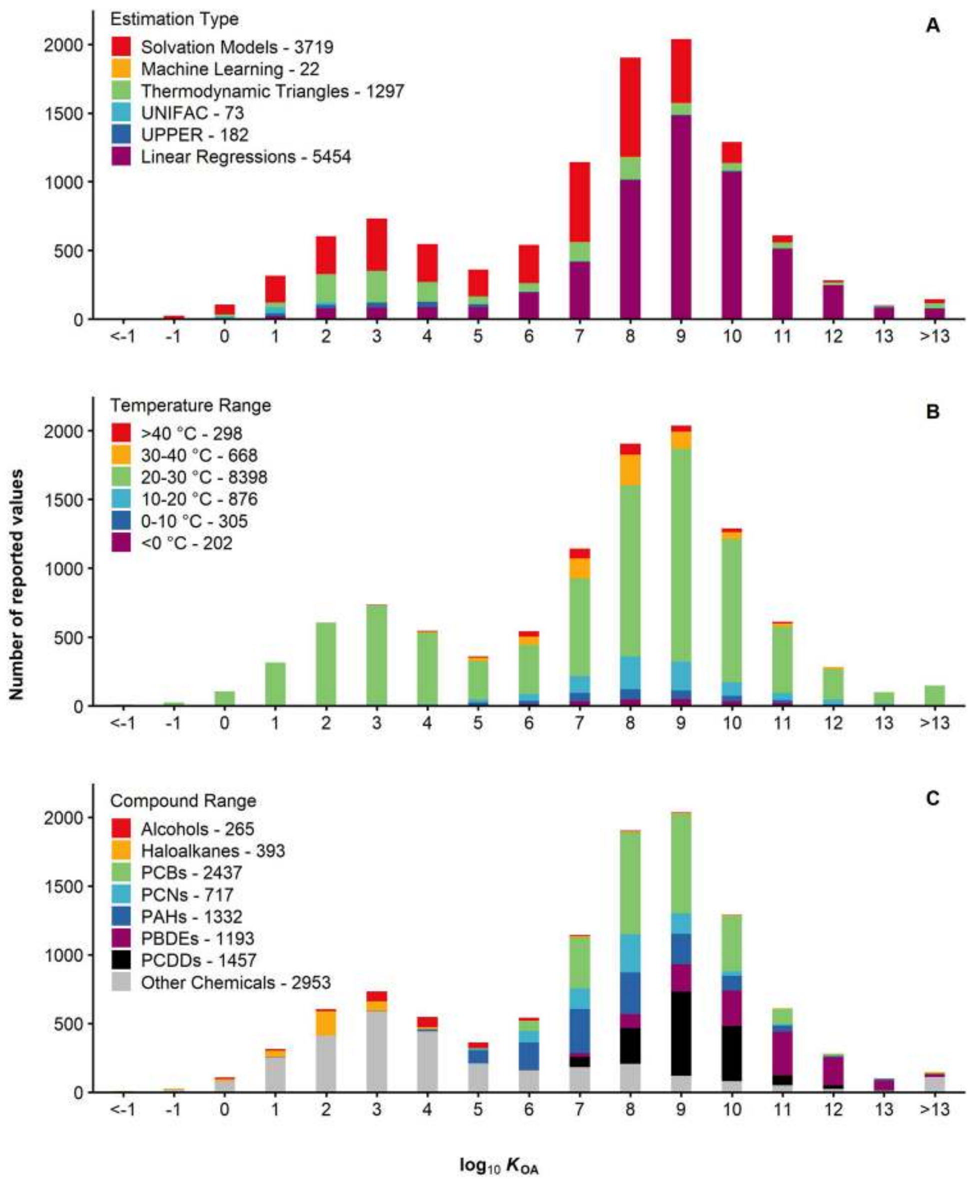

FIG. 9. Distribution of estimated $\log_{10} K_{OA}$ values included in the database. Each panel shows the distribution based on the estimation technique [Panel (a)], the temperature range of the reported value [(Panel (b)], and common classes of chemicals where estimated K_{OA} values exist [(Panel (c)].

TABLE 6. A summary of all papers and techniques that report estimated K_{OA} values included in the database, including the type of methodology and the $\log_{10} K_{OA}$ and temperature ranges for each method. The chemical classes used are not included as estimation models are not all intended for specific compound groups

References	Method	Technique	n	$\log_{10} K_{OA}$ range	Temperature range (°C)	Compound groups
Abraham *et al.* (2001)	Triangle	Thermodynamic triangles	23	4.46–9.59	25	PAHs, CBz, Hydrocarbons
Abraham *et al.* (2005)	MLR	Linear regressions	21	5.52–7.67	25	Methyl and alkyl substituted naphthalenes
Abraham *et al.* (2005)	MLR	Linear regressions	21	5.52–7.85	25	Methyl and alkyl substituted naphthalenes
Best *et al.* (1997)	Triangle	Thermodynamic triangles	66	−3.02–7.55	25	Diverse compounds
Best *et al.* (1997)	OPLS	Solvation models	63	−0.6–6.51	25	Diverse compounds
Best *et al.* (1997)	MMFF	Solvation models	66	0.05–6.66	25	Diverse compounds
Chen *et al.* (2001)	PLS	Linear regressions	33	7.08–12.46	25	PCDD/Fs
Chen *et al.* (2002a)	PLS	Linear regressions	57	7.4–11.66	−50–0	PCDD/Fs
Chen *et al.* (2002b)	PLS	Linear regressions	210	5.61–12.29	25	PCBs
Chen *et al.* (2003a)	PLS	Linear regressions	52	8.33–13.26	15–45	PBDEs
Chen *et al.* (2003b)	PLS	Linear regressions	97	6.73–12.76	−10–30	PCBs
Chen *et al.* (2003c)	PLS	Linear regressions	31	4.47–10.11	25	PCNs, CBz
Chen *et al.* (2016)	PLS	Linear regressions	208	6.3–12	25	PCBs
Chen *et al.* (2016)	PLS	Linear regressions	208	6.64–12.56	25	PCBs
Cousins and Mackay (2000)	LR	Linear regressions	22	7.01–13.01	25	Phthalate esters
Dallas (1995)	MOSCED	Solvation models	39	0.09–1.93	25	Simple hydrocarbons
Dallas (1995)	UNIFAC	UNIFAC	73	0.4–2.38	25	Simple hydrocarbons
Duffy and Jorgensen (2000)	MC	Linear regressions	85	−0.21–7.38	25	Simple diverse compounds
Ferreira (2001)	PLS	Linear regressions	16	5.01–14.09	25	PAHs
Finizio *et al.* (1997)	Triangle	Thermodynamic triangles	32	6.68–11.19	25	CBz, PCBs, DDT, PAHs, HCH
Fu *et al.* (2016)	SM8AD	Solvation models	376	−0.65–12.78	25	PCNs, PBDEs, PCBs, DDT, other hydrocarbons
Fu *et al.* (2016)	SM8AD	Solvation models	376	−0.65–12.78	25	PCNs, PBDEs, PCBs, DDT, other hydrocarbons
Giesen *et al.* (1997)	SM5.4/PM3	Solvation models	31	0.07–5.35	25	Diverse compounds
Giesen *et al.* (1997)	SM5.4/AM1	Solvation models	30	0.44–5.43	25	Diverse compounds
Hiatt (1997)	Triangle	Thermodynamic triangles	113	0.3–6.7	25	Hydrocarbons, PAHs, CBz, halogenated, amines, labeled
Jiao *et al.* (2014)	ANN	Machine learning	22	7.38–12.23	25	PBDEs
Jiao *et al.* (2017)	MLR	Linear regressions	22	7.4–12.26	25	PBDEs
Jin *et al.* (2017)	MLR	Linear regressions	98	4.63–11.5	−10–50	PAHs, CBz, PCNs, PCBs, PBDEs, PCDDS, etc.

TABLE 6. *(Continued)*

References	Method	Technique	n	$\log_{10} K_{OA}$ range	Temperature range (°C)	Compound groups
Kim *et al.* (2016)	SLR[a]	Linear regressions	76	7.28–12.07	25	PCDDs
Kim *et al.* (2016)	SLR[a]	Linear regressions	76	7.33–12.11	25	PCDDs
Kim *et al.* (2016)	SLR[a]	Linear regressions	76	7.33–12.11	25	PCDDs
Kim *et al.* (2016)	SLR[a]	Linear regressions	76	7.33–12.11	25	PCDDs
Kim *et al.* (2016)	SLR[a]	Linear regressions	76	7.33–12.11	25	PCDDs
Kim *et al.* (2016)	SLR[a]	Linear regressions	76	7.33–12.12	25	PCDDs
Kim *et al.* (2016)	SLR[a]	Linear regressions	76	7.34–12.11	25	PCDDs
Kim *et al.* (2016)	SLR[a]	Linear regressions	76	7.38–12.14	25	PCDDs
Kim *et al.* (2016)	SLR[a]	Linear regressions	76	7.51–12.26	25	PCDDs
Kim *et al.* (2016)	SLR[a]	Linear regressions	76	7.59–12.11	25	PCDDs
Kim *et al.* (2016)	SLR[a]	Linear regressions	76	7.59–12.34	25	PCDDs
Kim *et al.* (2016)	SLR[a]	Linear regressions	76	7.6–12.3	25	PCDDs
Kim *et al.* (2016)	SLR[a]	Linear regressions	76	7.74–12.26	25	PCDDs
Kim *et al.* (2016)	SLR[a]	Linear regressions	76	8.33–12.19	25	PCDDs
Kurz and Ballschmiter (1999)	Triangle	Thermodynamic triangles	107	6.33–9.13	25	PCDEs
Li *et al.* (1999)	SM5.4/PM3	Solvation models	192	−1.24–10.98	25	Diverse compounds
Li *et al.* (1999)	SM5.4/AM1	Solvation models	192	−1.24–11.48	25	Diverse compounds
Li *et al.* (2006)	MLR	Linear regressions	598	3.45–14.54	10–40	PAHs, CBz, PCNs, PCBs, PBDEs, PCDD/Fs
Li *et al.* (2020)	SMD/HF/MIDI!6D	Solvation models	836	6.22–10.89	10–30	Diverse compounds
Lian and Yalkowsky (2014)	UPPER	UPPER	170	1.15–15.63	25	Hydrocarbons, PAHs
Liu *et al.* (2013)	PLS	Linear regressions	39	8.43–13.3	25	PBDEs
Liu *et al.* (2013)	PLS	Linear regressions	39	8.7–13.29	25	PBDEs
Mathieu (2020)	MLR and PLS	Linear regressions	935	−0.38–13.78	−10–50	Diverse compounds
Meylan and Howard (2005)	Triangle	Thermodynamic triangles	434	−1.14–13.67	10–25	Various hydrocarbons
Nabi *et al.* (2014)	LFER	Linear regressions	52	4.1–10.56	25	Nonpolar organic compounds
Nabi *et al.* (2014)	ppLFER	Linear regressions	52	4.12–11.11	25	Nonpolar organic compounds
Nedyalkova *et al.* (2019)	M11	Solvation models	55	−0.4–7.3	25	Hydrocarbons
Nedyalkova *et al.* (2019)	B3LYP	Solvation models	55	−0.08–7.65	25	Hydrocarbons
Nedyalkova *et al.* (2019)	M06-2X	Solvation models	55	1.65–9.1	25	Hydrocarbons
Odabasi *et al.* (2006a)	Triangle	Thermodynamic triangles	14	6.23–13.67	25	PAHs
Oliferenko *et al.* (2004)	MLR	Linear regressions	47	−0.15–5.15	25	Aliphatic compounds
Papa *et al.* (2009)	OLS	Linear regressions	220	6.65–17.97	25	PBDEs, other hydrocarbons
Parnis *et al.* (2015)	COSMO	Solvation models	1060	4.65–11.57	−5–40	PAHs
Puzyn and Falandysz (2005)	PCR	Linear regressions	75	5.76–11.52	25	PCNs
Raevsky *et al.* (2006)	Triangle	Thermodynamic triangles	98	−1.11–8.93	25	Hydrocarbons, CBz, PAHs, etc.
Raevsky *et al.* 2006	Triangle	Thermodynamic triangles	98	−0.75–8.46	25	PAHs, CBz, hydrocarbons

TABLE 6. (*Continued*)

References	Method	Technique	n	$\log_{10} K_{OA}$ range	Temperature range (°C)	Compound groups
Sepassi and Yalkowsky (2007)	Triangle	Thermodynamic triangles	219	1.99–12.99	25	Hydrocarbons, PCBs, CBz, PAHs, etc.
Vikas and Chayawan (2015)	SLR[a]	Linear regressions	18	6.66–12.07	25	PCDD/Fs
Vikas and Chayawan (2015)	SLR[a]	Linear regressions	18	6.94–12.14	25	PCDD/Fs
Vikas and Chayawan (2015)	SLR[a]	Linear regressions	18	7.21–12.25	25	PCDD/Fs
Vikas and Chayawan (2015)	SLR[a]	Linear regressions	18	7.21–12.25	25	PCDD/Fs
Vikas and Chayawan (2015)	SLR[a]	Linear regressions	18	7.22–12.15	25	PCDD/Fs
Wang *et al.* (2008)	MLR	Linear regressions	209	7.38–15.26	25	PBDEs
Xu *et al.* (2007)	MLR	Linear regressions	209	7.17–15.73	25	PBDEs
Yalkowsky *et al.* (1994b)	UPPER	UPPER	12	2.74–5.76	25	CBz
Yuan *et al.* (2016)	PLS	Linear regressions	209	5.7–11.14	25	PCBs
Yuan *et al.* (2016)	MLR	Linear regressions	209	6.6–11.6	25	PCBs
Zeng *et al.* (2013)	MLR	Linear regressions	76	7.15–12.25	25	PCDDs
Zhang *et al.* (2016)	SPARC	Solvation models	93	2.6–28.4	25	Novel flame retardants
Zhang *et al.* (2016)	Triangle	Thermodynamic triangles	93	4.4–30.2	25	Novel flame retardants
Zhang *et al.* (2016)	ABSOLV	Linear regressions	93	5.6–29.1	25	Novel flame retardants
Zhao *et al.* (2005)	MLR	Linear regressions	6	4.44–6.91	25	PCNs
Zhao *et al.* (2005)	MLR	Linear regressions	4	6.83–8.86	25	CBs
Zhao *et al.* (2005)	MLR	Linear regressions	24	6.93–10.18	25	PBDES
Zhao *et al.* (2005)	MLR	Linear regressions	10	7.79–11.68	25	PAHs
Zhao *et al.* (2005)	MLR	Linear regressions	13	9.4–12.26	25	PCDD/Fs
Zhu *et al.* (1998)	SM5.42R/BPW91/MIDI!6D	Solvation models	192	−1.25–9.93	25	Diverse compounds
Zhu *et al.* (1998)	SM5.42R/BPW91/6-31G*	Solvation models	192	−1.24–9.91	25	Diverse compounds
Zhu *et al.* (1998)	SM5.42R/BPW91/DZVP	Solvation models	192	−1.21–9.95	25	Diverse compounds

[a]Different molecular descriptors are used to develop multiple single linear regressions models for K_{OA}.

GC-RT-derived $\log_{10} K_{OA}$ of hydrogen-bonding chemicals ($aA + bB > 0.5$) have unusually large residuals with all three prediction techniques, suggesting a large bias. Most residuals are negative, implying that the K_{OA} for such chemicals is biased low, which is consistent with expectations. We conclude that the GC-RT method is unsuitable for measuring the $\log_{10} K_{OA}$ of polar, and especially hydrogen-bonding, chemicals because (i) the interactions between the octanol and the reference chemical are not necessarily comparable to the interactions between octanol and the analyte of interest and (ii) the way the analyte interacts with the stationary phase will not be similar to its interaction with octanol due to the latter's capacity to undergo hydrogen bonding.

Within the database, we have noted which K_{OA} values obtained by GC-RT techniques may be erroneous due to the high polarity of the chemical.

4.7. Estimated K_{OA} values

The range of 10 747 estimated K_{OA} values in the literature is much larger than that of the experimentally derived values. The lowest estimated $\log_{10} K_{OA}$ value is −3.02 for propylnitrile (CAS No. 107-12-0) by Best *et al.* (1997) using a thermodynamic triangle approach based on ΔG°_{AW} and $\log_{10} K_{OW}$. The highest estimated $\log_{10} K_{OA}$ value, 30.20 for 1,2-bis[(2,3,4,5,6-pentabromophenyl) methyl] 3,4,5,6-tetrabromo-1,2-benzenedicarboxylate (CAS No. 82 001-21-6) by Zhang *et al.* (2016), was obtained using the thermodynamic triangle approach implemented in EPISuite's KOAWIN.

The general distribution of estimated K_{OA} values is similar to that of the experimentally derived values, with the majority of estimated values (70%) within the $\log_{10} K_{OA}$ 6–12 range (Fig. 9). A large portion of estimated $\log_{10} K_{OA}$ values are also in the 2–5 range (17.5%). Fewer estimates are made above $\log_{10} K_{OA}$ 13 (3.5%) or below 1 (1.3%). Between $\log_{10} K_{OA}$ 5 and 6, there are also few estimates (3.4%).

Half (50.7%) of the estimated values are derived from some form of linear regression, as described in Sec. 3.1.2. Solvation models for estimating K_{OA} are also very commonly used (34.6%), followed by thermodynamic triangle estimation techniques (12.0%). Both models are used across a broad K_{OA} range. Likewise, the UPPER model is not restricted to a specific range of chemicals because it is rooted in principles applied to thermodynamic triangles. However, estimates are not commonly available in the literature, and almost two thirds of published values obtained with UPPER (63.7%) fall within the $\log_{10} K_{OA}$ range between 1 and 5. The UNIFAC model is typically applied to estimate K_{OA} of volatile chemicals, and thus, reported values range only from 0.4 (tetrahydropyran; CAS No. 142-68-7) to 2.38 (dimethyl sulfoxide; CAS No. 67-68-5). Estimates made using machine learning techniques are limited to the work by Jiao *et al.* (2014) on PBDEs. As methods for estimating physical–chemical properties using neural networks and machine learning are developed further and because these approaches are not limited to a specific subset of chemicals, we expect their estimation range to widen significantly.

Most estimates are for $\log_{10} K_{OA}$ at 25 °C (71.9%). There are 3023 estimated K_{OA} values for 486 different chemicals at non-standard temperatures, which have been reported by nine publications using either linear regressions, thermodynamic triangles, or solvation models. Linear regression models use temperature-dependent experimental K_{OA} values for training and validation (Chen *et al.* 2003c, 2003b, 2002b; Li *et al.* 2006; Mathieu 2020). The descriptors for these models are temperature-dependent (e.g., X_i/T) because temperature and K_{OA} are inversely correlated. Meylan and Howard (2005) estimated the temperature dependence of K_{OA} from that of k_H, i.e., ignore the temperature dependence of K_{OW} during the application of the thermodynamic triangle of Eq. (10). Li *et al.* (2020) estimated a temperature-dependent K_{OA} by estimating ΔG°_{OA} at 25 °C using a solvation model and then solving Eq. (6) with different values of T. The assumption that ΔG°_{OA} is not strongly temperature-dependent is similar to assuming that ΔU_{OA} or ΔH_{OA} are weakly temperature-dependent. Some solvation models, such as COSMOtherm, can directly estimate ΔG°_{OA} at different temperatures (Parnis *et al.* 2015).

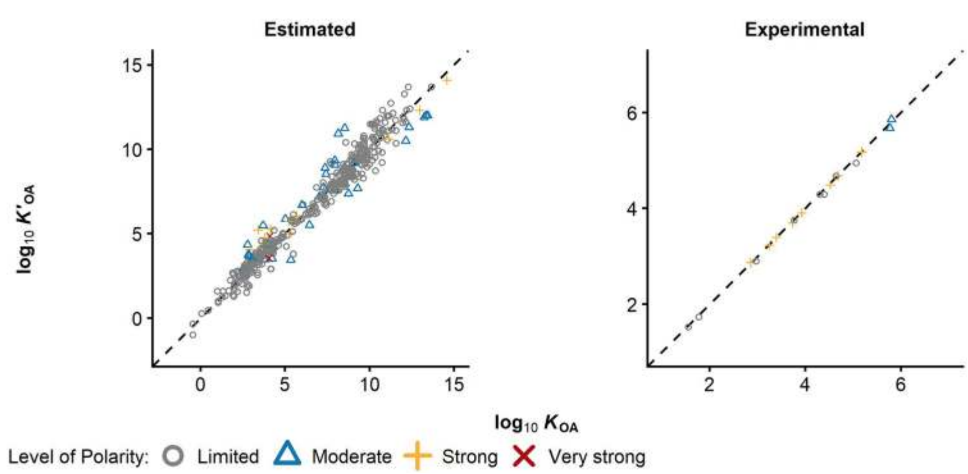

FIG. 10. Comparison of $\log_{10} K_{OA}$ and $\log_{10} K'_{OA}$ values for the same chemicals at the same temperature. The dashed lines have a slope of 1.

The chemical classes for which K_{OA} is commonly estimated reflect the availability of experimental data for K_{OA}. The most commonly estimated K_{OA} values are for PCBs (22.7%), PCDDs (13.6%), PAHs (12.4%), PBDEs (11.1%), and PCNs (0.7%) within the $\log_{10} K_{OA}$ 9–12 range. At the lower range of K_{OA} values, there are more estimates of alcohols and haloalkanes. There are also K_{OA} estimates for different CBz, arenes, alkanes, and OPEs. A full list of all methods and papers reporting estimated $\log_{10} K_{OA}$ values is included in Table 6.

4.8. Differences between K_{OA} and K'_{OA}

In Sec. 1.1.5, we remarked on the use of wet-octanol in place of dry-octanol. In Fig. 10, we compare the K_{OA} and K'_{OA} values for the same chemicals; however, there is no visible difference between the two K_{OA} values that can be attributed to the polarity of the compound. While there is a limited number of chemicals with both empirically derived K_{OA} and K'_{OA} values, the two sets of values are very similar. Estimated K_{OA} and K'_{OA} values are also well correlated, and the deviations seen could be attributed more toward differences in the estimation approach rather than the difference between wet- and dry-octanol. The effects of using wet-octanol will likely be more evident for more polar compounds at the higher $\log_{10} K_{OA}$ range, for which data currently is lacking.

5. Conclusions

The earliest K_{OA} data included in this work was published in 1960 by Boyer and Bircher. Following these first measurements, interest in K_{OA} waned for almost 30 years, likely due to the difficulty in measuring this property and the lack of direct applicability. In the 1990s, K_{OA} became of increasing interest due to its applicability in pharmaceutical and environmental chemistry and as technological advances and new analytical techniques were more widely accessible (Figs. SI 5–SI 7). The database assembled here is an effort to catalog the work of various researchers to measure and estimate K_{OA} and assess the applicability ranges of the different techniques used. The database currently includes 13 264 K_{OA} values for 1643 different chemicals. Of these, 2517 K_{OA} values are experimentally derived and the remaining 10 747 are estimated.

In almost all cases, the development of a new model or estimation technique for $\log_{10} K_{OA}$ requires good reference data that can be used to train and validate the model. Large training and validation datasets, including diverse chemicals, are necessary to generate robust models. We hope that this database will serve as a basis for new estimation techniques and experimental measurements of K_{OA} and as a reference dataset.

6. Supplementary Material

See the supplementary material for additional figures (Figs. SI 1–SI 7—the distribution of data with respect to time, methodology, reliability scores, and additional properties included in the database). A Microsoft Excel file containing the K_{OA} database is included.

Acknowledgments

We thank Tom Harner for sharing his K_{OA} measurement data with us. We thank Alessandro Sangion for his advice on database structure and formatting. We acknowledge the European Chemical Industry Council (CEFIC) for funding from Project No. ECO-41 of the Long-range Research Initiative (LRI).

List of Symbols

Within this work, we utilize a variety of variables and abbreviations. In some cases, the abbreviations have not been explicitly defined in the text. For convenience, we have included all abbreviations and variables here.

Variables

C_A	concentration in air
C_O	concentration in octanol
C_W	concentration in water
k_H	Henry's law constant in water
k_H^{oct}	Henry's law constant in octanol
$k_H'^{oct}$	reciprocal of Henry's law constant in octanol
K'_{OA}	wet octanol–air partition ratio
K_{AW}	air–water partition ratio
K_{OA}	octanol–air partition ratio
K_{OW}	octanol–water partition ratio
L_{oct}	Ostwald coefficient in octanol
P_L	liquid vapor pressure or subcooled liquid vapor pressure
v_{oct}	molar volume of octanol
γ_o^∞	activity coefficient at infinite dilution in octanol
ΔG°	Gibbs free energy
ΔG°_{OA}	Gibbs free energy of solvation in octanol
S_O	solubility in octanol

Compounds/compound groups

BFRs	brominated flame retardants
CBz	chlorobenzenes
DDT	dichlorodiphenyltrichloroethane
FOSA	perfluorinated alkyl sulfonamides
FOSE	perfluorinated sulfonamido ethanols
FTAs	fluorotelomer acrylates
FTOHs	fluorotelomer alcohols
HCH	hexachlorocyclohexane
OCPs	organochlorine pesticides
OPEs	organophosphate esters
POPs	persistent organic pollutants
PAHs	polycyclic aromatic hydrocarbons
PBDEs	polybrominated diphenyl ethers
PCBs	polychlorinated biphenyls
PCDD/Fs	polychlorinated dibenzodioxins and polychlorinated dibenzofurans
PCDDs	polychlorinated dibenzodioxins
PCDEs	polychlorinated diphenyl ether

PCDFs	polychlorinated dibenzofurans
PCNs	polychlorinated naphthalenes
PFASs	per/poly-fluoroalkyl substances
VOCs	volatile organic compounds

Experimental/estimation techniques

2P-Eqbm	two-phase equilibrium technique
3P-Eqbm	three-phase equilibrium technique
ABSOLV	ACD/ABSOLV program from ACD/Labs
ANN	artificial neural network
B3LYP	parameterization condition of a solvation model
BN-B	Ben-Naim/Baer-type apparatus
CoMFA	comparative molecular field analysis
CoMSIA	comparative molecular similarity indices analysis
COSMO	conductor-like screening model
Dynamic	dynamic techniques
FM	fugacity meter or generator column
GasSol	gas solubility
GC-RT	gas chromatography retention time
GLC-RT	gas–liquid chromatography retention time
GS	gas stripping
HS	headspace
HS and GC	headspace with gas chromatography
HS Vac	headspace with vacuum
LFER	linear free energy relationship
LR	linear regression
M06-2X	parameterization condition of a solvation model
M11	parameterization condition of a solvation model
MA	modified Morrison–Billett apparatus
MC	Monte Carlo analysis
MCIs	molecular connectivity indexes
MLR	multiple linear regression
MMFF	parameterization condition of a solvation model
MOSCED	modified separation of cohesive energy density model
MR-GC-RT	multi reference gas chromatography retention time
MR-SC-GC-RT	multi reference, single column, gas chromatography retention time
OLS	ordinary least squares
OPLS	optimized potentials for liquid simulations force field—the parameterization used in the continuum solvation model
PCR	principal component regression
PLS	partial least squares
PM	photomultiplier
ppLFER	poly-parameter linear free energy relationships
PP	partial pressure technique
QSARs	quantitative structure–activity relationships
QSPRs	quantitative structure–property relationships
RT	retention time
RTI	retention time index
SC-GC-RT	single reference, gas chromatography retention time
SLR	single linear regression
SM5.4/AM1	parameterization condition of a solvation model
SM5.4/PM3	parameterization condition of a solvation model
SM5.42R/BPW91/6-31G*	parameterization condition of a solvation model
SM5.42R/BPW91/DZVP	parameterization condition of a solvation model
SM5.42R/BPW91/MIDI!6D	parameterization condition of a solvation model
SM8AD	parameterization condition of a solvation model
SMD/HF/MIDI!6D	parameterization condition of a solvation model
SPARC	SPARC performs automated reasoning in chemistry, software by ARChem
SPME	solid phase microextraction
SR-GC-RT	single reference, gas chromatography retention time
Triangle	thermodynamic triangle techniques
UNIFAC	UNIQUAC functional-group activity coefficients
UNIQUAC	universal quasichemical
UPPER	unified physical property estimation relationship
VD/GC/MS	vacuum distillation gas chromatography mass spectrometry
Vgas	Van Slyke–Neill blood gas apparatus
VPHS	variable phase ratio

7. Data Availability

The data that support the findings of this study are openly available on GitHub (https://github.com/sivanibaskaran/koadata) and are available within its supplementary material.

8. References

Åberg, A., MacLeod, M., and Wiberg, K., “Physical–chemical property data for dibenzo-*p*-dioxin (DD), dibenzofuran (DF), and chlorinated DD/Fs: A critical review and recommended values,” J. Phys. Chem. Ref. Data **37**, 1997–2008 (2008).

Abraham, M. H. and Acree, W. E., “Comparison of solubility of gases and vapours in wet and dry alcohols, especially octan-1-ol,” J. Phys. Org. Chem. **21**, 823–832 (2008).

Abraham, M. H. and Acree, W. E., “Descriptors for the prediction of partition coefficients and solubilities of organophosphorus compounds,” Sep. Sci. Technol. **48**, 884–897 (2013).

Abraham, M. H. and Al-Hussaini, A. J. M., "Solvation descriptors for the polychloronaphthalenes: Estimation of some physicochemical properties," J. Environ. Monit. **3**, 377–381 (2001).

Abraham, M. H. and Al-Hussaini, A. J. M., "Solvation descriptors for *N*-nitrosodialkylamines; calculation of some of their properties of environmental significance," J. Environ. Monit. **4**, 743–746 (2002).

Abraham, M. H., Autenrieth, R., and Dimitriou-Christidis, P., "The estimation of physicochemical properties of methyl and other alkyl naphthalenes," J. Environ. Monit. **7**, 445–449 (2005).

Abraham, M. H., Le, J., Acree, W. E., Carr, P. W., and Dallas, A. J., "The solubility of gases and vapours in dry octan-1-ol at 298 K," Chemosphere **44**, 855–863 (2001).

Abraham, M. H., Nasezadeh, A., and Acree, W. E., "Correlation and prediction of partition coefficients from the gas phase and from water to alkan-1-ols," Ind. Eng. Chem. Res. **47**, 3990–3995 (2008).

Alarie, Y., Nielsen, G. D., Andonian-Haftvan, J., Abraham, M. H., "Physicochemical properties of nonreactive volatile organic chemicals to estimate RD50: Alternatives to animal studies," Toxicol. Appl. Pharmacol. **134**, 92–99 (1995).

Atkinson, D. and Curthoys, G., "The determination of heats of adsorption by gas-solid chromatography," J. Chem. Educ. **55**, 564 (1978).

Batterman, S., Zhang, L., Wang, S., and Franzblau, A., "Partition coefficients for the trihalomethanes among blood, urine, water, milk and air," Sci. Total Environ. **284**, 237–247 (2002).

Battino, R., "The Ostwald coefficient of gas solubility," Fluid Phase Equilib. **15**, 231–240 (1984).

Battino, R. and Clever, H. L., "The solubility of gases in liquids," Chem. Rev. **66**, 395–463 (1966).

Berti, P., Cabani, S., Conti, G., and Mollica, V., "Thermodynamic study of organic compounds in octan-1-ol. Processes of transfer from gas and from dilute aqueous solution," J. Chem. Soc., Faraday Trans. 1 **82**, 2547–2556 (1986).

Best, S. A., Merz, K. M., and Reynolds, C. H., "GB/SA-based continuum solvation model for octanol," J. Phys. Chem. B **101**, 10479–10487 (1997).

Beyer, A., Wania, F., Gouin, T., Mackay, D., and Matthies, M., "Selecting internally consistent physicochemical properties of organic compounds," Environ. Toxicol. Chem. **21**, 941–953 (2002).

Bhatia, S. R. and Sandler, S. I., "Temperature dependence of infinite dilution activity coefficients in octanol and octanol/water partition coefficients of some volatile halogenated organic compounds," J. Chem. Eng. Data **40**, 1196–1198 (1995).

Bo, S., Battino, R., and Wilhelm, E., "Solubility of gases in liquids. 19. Solubility of He, Ne, Ar, Kr, Xe, N_2, O_2, CH_4, CF_4, and SF_6 in normal 1-alkanols n-$C_lH_{2l+1}OH$ ($1 < l < 11$) at 298.15 K," J. Chem. Eng. Data **38**, 611–616 (1993).

Boyer, F. L. and Bircher, L. J., "The solubility of nitrogen, argon, methane, ethylene and ethane in normal primary alcohols," J. Phys. Chem. **64**, 1330–1331 (1960).

Brown, T. N., "Predicting hexadecane–air equilibrium partition coefficients (L) using a group contribution approach constructed from high quality data," SAR QSAR Environ. Res. **25**, 51–71 (2014).

Brown, T. N., Arnot, J. A., and Wania, F., "Iterative fragment selection: A group contribution approach to predicting fish biotransformation half-lives," Environ. Sci. Technol. **46**, 8253–8260 (2012).

Cabani, S., Conti, G., Mollica, V., and Bernazzani, L., "Free energy and enthalpy changes for the process of transfer from gas and from dilute aqueous solutions of some alkanes and monofunctional saturated organic compounds," J. Chem. Soc. Faraday Trans. **87**, 2433–2442 (1991).

Castells, C. B., Carr, P. W., Eikens, D. I., Bush, D., and Eckert, C. A., "Comparative study of semitheoretical models for predicting infinite dilution activity coefficients of alkanes in organic solvents," Ind. Eng. Chem. Res. **38**, 4104–4109 (1999).

Chen, J., Harner, T., Ding, G., Quan, X., Schramm, K.-W., and Kettrup, A., "Universal predictive models on octanol–air partition coefficients at different temperatures for persistent organic pollutants," Environ. Toxicol. Chem. **23**, 2309 (2004).

Chen, J., Xue, X., Schramm, K.-W., Quan, X., Yang, F., and Kettrup, A., "Quantitative structure–property relationships for octanol–air partition coefficients of polychlorinated biphenyls," Chemosphere **48**, 535–544 (2002a).

Chen, J., Xue, X., Schramm, K.-W., Quan, X., Yang, F., and Kettrup, A., "Quantitative structure-property relationships for octanol–air partition coefficients of polychlorinated naphthalenes, chlorobenzenes and p,p'-DDT," Comput. Biol. Chem. **27**, 165–171 (2003a).

Chen, J. W., Harner, T., Schramm, K.-W., Quan, X., Xue, X. Y., and Kettrup, A., "Quantitative relationships between molecular structures, environmental temperatures and octanol–air partition coefficients of polychlorinated biphenyls," Comput. Biol. Chem. **27**, 405–421 (2003b).

Chen, J. W., Harner, T., Schramm, K.-W., Quan, X., Xue, X. Y., Wu, W. Z., and Kettrup, A., "Quantitative relationships between molecular structures, environmental temperatures and octanol–air partition coefficients of PCDD/Fs," Sci. Total Environ. **300**, 155–166 (2002b).

Chen, J. W., Harner, T., Yang, P., Quan, X., Chen, S., Schramm, K.-W., and Kettrup, A., "Quantitative predictive models for octanol–air partition coefficients of polybrominated diphenyl ethers at different temperatures," Chemosphere **51**, 577–584 (2003c).

Chen, J. W., Quan, X., Zhao, Y. Z., Yang, F. L., Schramm, K.-W., and Kettrup, A., "Quantitative structure–property relationships for octanol-air partition coefficients of PCDD/Fs," Bull. Environ. Contam. Toxicol. **66**, 755–761 (2001).

Chen, Y., Cai, X., Jiang, L., and Li, Y., "Prediction of octanol-air partition coefficients for polychlorinated biphenyls (PCBs) using 3D-QSAR models," Ecotoxicol. Environ. Saf. **124**, 202–212 (2016).

Cheong, W. J., "Measurements of limiting activity coefficients of homologous series of solutes and their application to the study of retention mechanism in reversed phase liquid chromatography," Ph.D. thesis, University of Minnesota, Minnesota, 1989.

Cousins, I. and Mackay, D., "Correlating the physical–chemical properties of phthalate esters using the 'three solubility' approach," Chemosphere **41**, 1389–1399 (2000).

Dallas, A. J., "Fundamental solvatochromic and thermodynamic studies of complex chromatographic media," Ph.D. thesis, University of Minnesota, Minnesota, 1995.

Dallas, A. J. and Carr, P. W., "A thermodynamic and solvatochromic investigation of the effect of water on the phase-transfer properties of octan-1-ol," J. Chem. Soc. Perkin Trans. **2**, 2155–2161 (1992).

Deanda, F., Smith, K. M., Liu, J., and Pearlman, R. S., "GSSI, a general model for solute–solvent interactions. 1. Description of the model," Mol. Pharm. **1**, 23–39 (2004).

Dreyer, A., Langer, V., and Ebinghaus, R., "Determination of octanol–air partition coefficients (K_{OA}) of fluorotelomer acrylates, perfluoroalkyl sulfonamids, and perfluoroalkylsulfonamido ethanols," J. Chem. Eng. Data **54**, 3022–3025 (2009).

Duffy, E. M. and Jorgensen, W. L., "Prediction of properties from simulations: Free energies of solvation in hexadecane, octanol, and water," J. Am. Chem. Soc. **122**, 2878–2888 (2000).

Eger, E. I., Halsey, M. J., Koblin, D. D., Laster, M. J., Ionescu, P., Königsberger, K., Fan, R., Nguyen, B. V., and Hudlicky, T., "The convulsant and anesthetic properties of cis-trans isomers of 1,2-dichlorohexafluorocyclobutane and 1,2-dichloroethylene," Anesth. Analg. **93**, 922–927 (2001).

Eger, E. I., Ionescu, P., Laster, M. J., Gong, D., Hudlicky, T., Kendig, J. J., Harris, R. A., Trudell, J. R., and Pohorille, A., "Minimum alveolar anesthetic concentration of fluorinated alkanols in rats: Relevance to theories of narcosis," Anesth. Analg. **88**, 867–876 (1999).

Eger, E. I., Koblin, D. D., Laster, M. J., Schurig, V., Juza, M., Ionescu, P., and Gong, D., "Minimum alveolar anesthetic concentration values for the enantiomers of isoflurane differ minimally," Anesth. Analg. **85**, 188–192 (1997).

Eikens, D. I., "Applicability of theoretical and semi-empirical models for predicting infinite dilution activity coefficients," Ph.D. Dissertation (University of Minnesota, Minnesota, 1993).

Endo, S. and Goss, K.-U., "Applications of polyparameter linear free energy relationships in environmental chemistry," Environ. Sci. Technol. **48**, 12477–12491 (2014).

Endo, S. and Hammer, J., "Predicting partition coefficients of short-chain chlorinated paraffin congeners by COSMO-RS-trained fragment contribution models," Environ. Sci. Technol. **54**, 15162–15169 (2020).

EPI Suite Data (4.11), (Microsoft® Windows), United States Environmental Protection Agency, 2012, https://www.epa.gov/tsca-screening-tools/epi-suitetm-estimation-program-interface.

Ettre, L. S., Welter, C., and Kolb, B., "Determination of gas–liquid partition coefficients by automatic equilibrium headspace-gas chromatography utilizing the phase ratio variation method," Chromatographia **35**, 73–84 (1993).

Fang, Z., Ionescu, P., Chortkoff, B. S., Kandel, L., Sonner, J., Laster, M. J., and Eger, E. I., "Anesthetic potencies of *n*-alkanols: Results of additivity and solubility studies suggest a mechanism of action similar to that for conventional inhaled anesthetics," Anesth. Analg. **84**, 1042–1048 (1997a).

Fang, Z., Laster, M. J., Gong, D., Ionescu, P., Koblin, D. D., Sonner, J., Eger, E. I., and Halsey, M. J., "Convulsant activity of nonanesthetic gas combinations," Anesth. Analg. **84**, 634–640 (1997b).

Fang, Z., Sonner, J., Laster, M. J., Ionescu, P., Kandel, L., Koblin, D. D., Eger II, E. I., and Halsey, M. J., "Anesthetic and convulsant properties of aromatic compounds and cycloalkanes: Implications for mechanisms of narcosis," Anesth. Analg. **83**, 1097–1104 (1996).

Ferreira, M. M. C., "Polycyclic aromatic hydrocarbons: A QSPR study," Chemosphere **44**, 125–146 (2001).

Finizio, A., Mackay, D., Bidleman, T., and Harner, T., "Octanol-air partition coefficient as a predictor of partitioning of semi-volatile organic chemicals to aerosols," Atmos. Environ. **31**, 2289–2296 (1997).

Fredenslund, A., Jones, R. L., and Prausnitz, J. M., "Group-contribution estimation of activity coefficients in nonideal liquid mixtures," AIChE J. **21**, 1086–1099 (1975).

Fu, Z., Chen, J., Li, X., Wang, Y., and Yu, H., "Comparison of prediction methods for octanol-air partition coefficients of diverse organic compounds," Chemosphere **148**, 118–125 (2016).

Fuchs, R. and Stephenson, W. K., "Enthalpies of transfer of alkane solutes from the vapor state to organic solvents," Can. J. Chem. **63**, 349–352 (1985).

Fukuchi, K., Miyoshi, K., Watanabe, T., Yonezawa, S., and Arai, Y., "Measurement and correlation of infinite dilution activity coefficients of ethers in alkanols," Fluid Phase Equilib. **156**, 197–206 (1999).

Fukuchi, K., Miyoshi, K., Watanabe, T., Yonezawa, S., and Arai, Y., "Measurement and correlation of infinite dilution activity coefficients of bis(2,2,2-trifluoroethyl)ether in dodecane or alkanol," Fluid Phase Equilib. **182**, 257–263 (2001).

Giesen, D. J., Hawkins, G. D., Liotard, D. A., Cramer, C. J., and Truhlar, D. G., "A universal model for the quantum mechanical calculation of free energies of solvation in non-aqueous solvents," Theor. Chem. Acc. **98**, 85–109 (1997).

Goss, K.-U., Bronner, G., Harner, T., Hertel, M., and Schmidt, T. C., "The partition behavior of fluorotelomer alcohols and olefins," Environ. Sci. Technol. **40**, 3572–3577 (2006).

Goss, K.-U. and Eisenreich, S. J., "Adsorption of VOCs from the gas phase to different minerals and a mineral mixture," Environ. Sci. Technol. **30**, 2135–2142 (1996).

Gruber, D., Langenheim, D., Gmehling, J., and Moollan, W., "Measurement of activity coefficients at infinite dilution using gas–liquid chromatography. 6. Results for systems exhibiting gas–liquid interface adsorption with 1-octanol," J. Chem. Eng. Data **42**, 882–885 (1997).

Ha, Y. and Kwon, J.-H., "Determination of 1-octanol-air partition coefficient using gaseous diffusion in the air boundary layer," Environ. Sci. Technol. **44**, 3041–3046 (2010).

Harner, T. and Bidleman, T. F., "Measurements of octanol–air partition coefficients for polychlorinated biphenyls," J. Chem. Eng. Data **41**, 895–899 (1996).

Harner, T. and Bidleman, T. F., "Measurement of octanol–air partition coefficients for polycyclic aromatic hydrocarbons and polychlorinated naphthalenes," J. Chem. Eng. Data **43**, 40–46 (1998).

Harner, T., Green, N. J. L., and Jones, K. C., "Measurements of octanol–air partition coefficients for PCDD/Fs: A tool in assessing air–soil equilibrium status," Environ. Sci. Technol. **34**, 3109–3114 (2000).

Harner, T. and Mackay, D., "Measurement of octanol-air partition coefficients for chlorobenzenes, PCBs, and DDT," Environ. Sci. Technol. **29**, 1599–1606 (1995).

Harner, T. and Shoeib, M., "Measurements of octanol–air partition coefficients (K_{OA}) for polybrominated diphenyl ethers (PBDEs): predicting partitioning in the environment," J. Chem. Eng. Data **47**, 228–232 (2002).

Hiatt, M. H., "Vacuum distillation coupled with gas chromatography/mass spectrometry for the analysis of environmental samples," Anal. Chem. **67**, 4044–4052 (1995).

Hiatt, M. H., "Analyses of fish tissue by vacuum distillation/gas chromatography/mass spectrometry," Anal. Chem. **69**, 1127–1134 (1997).

Hiatt, M. H., "Bioconcentration factors for volatile organic compounds in vegetation," Anal. Chem. **70**, 851–856 (1998).

Hilal, S. H., Karickhoff, S. W., and Carreira, L. A., "Verification and validation of the SPARC model," U.S. Environmental Protection Agency, Washington, D.C., EPA/600/R-03/033 (NTIS PB2004-101168), 2003, https://cfpub.epa.gov/si/si_public_record_report.cfm?Lab=NERL & dirEntryId=63414.

Hippelein, M. and McLachlan, M. S., "Soil/air partitioning of semivolatile organic compounds. 1. Method development and influence of physical–chemical properties," Environ. Sci. Technol. **32**, 310–316 (1998).

Hippelein, M. and McLachlan, M. S., "Soil/air partitioning of semivolatile organic compounds. 2. Influence of temperature and relative humidity," Environ. Sci. Technol. **34**, 3521–3526 (2000).

Hussam, A. and Carr, P. W., "Rapid and precise method for the measurement of vapor/liquid equilibria by headspace gas chromatography," Anal. Chem. **57**, 793–801 (1985).

Ionescu, P., Eger, E. I., and Trudell, J., "Direct determination of oil/saline partition coefficients," Anesth. Analg. **79**, 1056–1058 (1994).

Jiao, L., Gao, M., Wang, X., and Li, H., "QSPR study on the octanol/air partition coefficient of polybrominated diphenyl ethers by using molecular distance-edge vector index," Chem. Cent. J. **8**, 36 (2014).

Jin, X., Fu, Z., Li, X., and Chen, J., "Development of polyparameter linear free energy relationship models for octanol–air partition coefficients of diverse chemicals," Environ. Sci.: Processes Impacts **19**, 300–306 (2017).

Kim, J., Mackay, D., and Powell, D. E., "Roles of steady-state and dynamic models for regulation of hydrophobic chemicals in aquatic systems: A case study of decamethylcyclopentasiloxane (D5) and PCB-180 in three diverse ecosystems," Chemosphere **175**, 253–268 (2017).

Kim, M., Li, L. Y., and Grace, J. R., "Predictability of physicochemical properties of polychlorinated dibenzo-*p*-dioxins (PCDDs) based on single-molecular descriptor models," Environ. Pollut. **213**, 99–111 (2016).

Klamt, A., "The COSMO and COSMO-RS solvation models," Wiley Interdiscip. Rev.: Comput. Mol. Sci. **1**, 699–709 (2011).

Klamt, A., "The COSMO and COSMO-RS solvation models," Wiley Interdiscip. Rev.: Comput. Mol. Sci. **8**, e1338 (2018).

Klamt, A., Eckert, F., and Diedenhofen, M., "Prediction or partition coefficients and activity coefficients of two branched compounds using COSMOtherm," Fluid Phase Equilib. **285**, 15–18 (2009).

Kömp, P. and McLachlan, M. S., "Octanol/air partitioning of polychlorinated biphenyls," Environ. Toxicol. Chem. **16**, 2433–2437 (1997).

Kurz, J. and Ballschmiter, K., "Vapour pressures, aqueous solubilities, Henry's law constants, partition coefficients between gas/water (K_{gw}), *n*-octanol/water (K_{ow}) and gas/*n*-octanol (K_{go}) of 106 polychlorinated diphenyl ethers (PCDE)," Chemosphere **38**, 573–586 (1999).

Lee, H.-J. and Kwon, J.-H., "Evaluation of long-range transport potential of selected brominated flame retardants with measured 1-octanol–air partition coefficients," Bull. Korean Chem. Soc. **37**, 1696–1702 (2016).

Lei, Y. D., Baskaran, S., and Wania, F., "Measuring the octan-1-ol air partition coefficient of volatile organic chemicals with the variable phase ratio headspace technique," J. Chem. Eng. Data **64**, 4793–4800 (2019).

Lei, Y. D., Wania, F., Mathers, D., and Mabury, S. A., "Determination of vapor pressures, octanol–air, and water–air partition coefficients for polyfluorinated sulfonamide, sulfonamidoethanols, and telomer alcohols," J. Chem. Eng. Data **49**, 1013–1022 (2004).

Leng, C.-B., Roberts, J. E., Zeng, G., Zhang, Y.-H., and Liu, Y., "Effects of temperature, pH, and ionic strength on the Henry's law constant of triethylamine," Geophys. Res. Lett. **42**, 3569–3575, https://doi.org/10.1002/2015GL063840 (2015).

Leo, A., Hansch, C., and Elkins, D., "Partition coefficients and their uses," Chem. Rev. **71**, 525–616 (1971).

Lerol, J.-C., Masson, J.-C., Renon, H., Fabries, J.-F., and Sannier, H., "Accurate measurement of activity coefficient at infinite dilution by inert gas stripping and gas chromatography," Ind. Eng. Chem. Process Des. Dev. **16**, 139–144 (1977).

Li, A., Pinsuwan, S., and Yalkowsky, S. H., "Estimation of solubility of organic compounds in 1-octanol," Ind. Eng. Chem. Res. **34**, 915–920 (1995).

Li, J., Zhu, T., Hawkins, G. D., Winget, P., Liotard, D. A., Cramer, C. J., and Truhlar, D. G., "Extension of the platform of applicability of the SM5.42R universal solvation model," Theor. Chem. Acc. **103**, 9–63 (1999).

Li, N., Wania, F., Lei, Y. D., and Daly, G. L., "A comprehensive and critical compilation, evaluation, and selection of physical–chemical property data for selected polychlorinated biphenyls," J. Phys. Chem. Ref. Data **32**, 1545–1590 (2003).

Li, X., Chen, J., Zhang, L., Qiao, X., and Huang, L., "The fragment constant method for predicting octanol–air partition coefficients of persistent organic pollutants at different temperatures," J. Phys. Chem. Ref. Data **35**, 1365–1384 (2006).

Li, Y.-F., Qiao, L.-N., Ren, N.-Q., Macdonald, R. W., and Kannan, K., "Gas/particle partitioning of semi-volatile organic compounds in the atmosphere: Transition from unsteady to steady state," Sci. Total Environ. **710**, 136394 (2020).

Li, Z.-H., Chen, G., Chen, Z.-T., Xia, Z.-N., Cheng, F.-S., and Chen, H., "Three-dimensional holographic vector of atomic interaction field (3D-HoVAIF) for the QSPR/QSAR of polychlorinated naphthalenes," Chin. J. Struct. Chem. **31**, 345–352 (2012).

Lian, B. and Yalkowsky, S. H., "Unified physicochemical property estimation relationships (UPPER)," J. Pharm. Sci. **103**, 2710–2723 (2014).

Liu, H., Shi, J., Liu, H., and Wang, Z., "Improved 3D-QSPR analysis of the predictive octanol–air partition coefficients of hydroxylated and methoxylated polybrominated diphenyl ethers," Atmos. Environ. **77**, 840–845 (2013).

Ma, Y.-G., Lei, Y. D., Xiao, H., Wania, F., and Wang, W.-H., "Critical review and recommended values for the physical-chemical property data of 15 polycyclic aromatic hydrocarbons at 25 °C," J. Chem. Eng. Data **55**, 819–825 (2010).

Mackay, D., Celsie, A. K. D., and Parnis, J. M., "The evolution and future of environmental partition coefficients," Environ. Rev. **24**, 101–113 (2015).

Mackay, D. and Shiu, W. Y., "A critical review of Henry's law constants for chemicals of environmental interest," J. Phys. Chem. Ref. Data **10**, 1175–1199 (1981).

Mackay, D., Shiu, W.-Y., and Lee, S. C., *Handbook of Physical–Chemical Properties and Environmental Fate for Organic Chemicals*, 2nd ed. (CRC Press, Boca Raton, FL, 2006).

Mansouri, K., Grulke, C. M., Judson, R. S., and Williams, A. J., "OPERA models for predicting physicochemical properties and environmental fate endpoints," J. Cheminformatics **10**, 10 (2018).

Mansouri, K. and Williams, A., "K_{OA} model for the octanol/air partition coefficient prediction from OPERA models," QMRF ID: Q17-18-0018, 2017.

Marenich, A. V., Cramer, C. J., and Truhlar, D. G., "Universal solvation model based on the generalized Born approximation with asymmetric descreening," J. Chem. Theory Comput. **5**, 2447–2464 (2009a).

Marenich, A. V., Cramer, C. J., and Truhlar, D. G., "Universal solvation model based on solute electron density and on a continuum model of the solvent defined by the bulk dielectric constant and atomic surface tensions," J. Phys. Chem. B **113**, 6378–6396 (2009b).

Mathieu, D., "QSPR versus fragment-based methods to predict octanol-air partition coefficients: Revisiting a recent comparison of both approaches," Chemosphere **245**, 125584 (2020).

Meylan, W. M. and Howard, P. H., "Estimating octanol-air partition coefficients with octanol–water partition coefficients and Henry's law constants," Chemosphere **61**, 640–644 (2005).

Mintz, C., Burton, K., Ladlie, T., Clark, M., Acree, W. E., and Abraham, M. H., "Enthalpy of solvation correlations for gaseous solutes dissolved in dibutyl ether and ethyl acetate," Thermochim. Acta **470**, 67–76 (2008).

Mintz, C., Clark, M., Acree, W. E., and Abraham, M. H., "Enthalpy of solvation correlations for gaseous solutes dissolved in water and in 1-octanol based on the Abraham model," J. Chem. Inf. Model. **47**, 115–121 (2007).

Müller, J. F., Hawker, D. W., and Connell, D. W., "Calculation of bioconcentration factors of persistent hydrophobic compounds in the air/vegetation system," Chemosphere **29**, 623–640 (1994).

Nabi, D., Gros, J., Dimitriou-Christidis, P., and Arey, J. S., "Mapping environmental partitioning properties of nonpolar complex mixtures by use of GC × GC," Environ. Sci. Technol. **48**, 6814–6826 (2014).

Nedyalkova, M. A., Madurga, S., Tobiszewski, M., and Simeonov, V., "Calculating the partition coefficients of organic solvents in octanol/water and octanol/air," J. Chem. Inf. Model. **59**, 2257–2263 (2019).

O'Boyle, N. M., Banck, M., James, C. A., Morley, C., Vandermeersch, T., and Hutchison, G. R., "Open Babel: An open chemical toolbox," J. Cheminformatics **3**, 33 (2011).

Ockenden, W. A., Sweetman, A. J., Prest, H. F., Steinnes, E., and Jones, K. C., "Toward an understanding of the global atmospheric distribution of persistent organic pollutants: The use of semipermeable membrane devices as time-integrated passive samplers," Environ. Sci. Technol. **32**, 2795–2803 (1998).

Odabasi, M. and Cetin, B., "Determination of octanol–air partition coefficients of organochlorine pesticides (OCPs) as a function of temperature: Application to air–soil exchange," J. Environ. Manage. **113**, 432–439 (2012).

Odabasi, M., Cetin, E., and Sofuoglu, A., "Determination of octanol–air partition coefficients and supercooled liquid vapor pressures of PAHs as a function of temperature: Application to gas–particle partitioning in an urban atmosphere," Atmos. Environ. **40**, 6615–6625 (2006a).

Odabasi, M., Cetin, B., and Sofuoglu, A., "Henry's law constant, octanol–air partition coefficient and supercooled liquid vapor pressure of carbazole as a function of temperature: Application to gas/particle partitioning in the atmosphere," Chemosphere **62**, 1087–1096 (2006b).

Okeme, J. O., Rodgers, T. F. M., Parnis, J. M., Diamond, M. L., Bidleman, T. F., and Jantunen, L. M., "Gas chromatographic estimation of vapor pressures and octanol–air partition coefficients of semivolatile organic compounds of emerging concern," J. Chem. Eng. Data **65**, 2467–2475 (2020).

Oliferenko, A. A., Oliferenko, P. V., Huddleston, J. G., Rogers, R. D., Palyulin, V. A., Zefirov, N. S., and Katritzky, A. R., "Theoretical scales of hydrogen bond acidity and basicity for application in QSAR/QSPR studies and drug design. Partitioning of aliphatic compounds," J. Chem. Inf. Comput. Sci. **44**, 1042–1055 (2004).

Ostwald, W., *Solutions* (Longmans Green & Co., London, UK; New York, 1891) (Translation: M. M. P. Muir), http://archive.org/details/solutions00ostwgoog.

Özcan Ç., "Determination of gas-particle partitioning parameters and indoor air concentrations of synthetic musk compounds," M.Sc. thesis, Izmir Institute of Technology, Izmir, Turkey, 2013, https://openaccess.iyte.edu.tr/handle/11147/3588.

Papa, E., Kovarich, S., and Gramatica, P., "Development, validation and inspection of the applicability domain of QSPR models for physicochemical properties of polybrominated diphenyl ethers," QSAR Comb. Sci. **28**, 790–796 (2009).

Park, J. H., Hussam, A., Couasnon, P., Fritz, D., and Carr, P. W., "Experimental reexamination of selected partition coefficients from Rohrschneider's data set," Anal. Chem. **59**, 1970–1976 (1987).

Parnis, J. M., Mackay, D., and Harner, T., "Temperature dependence of Henry's law constants and K_{OA} for simple and heteroatom-substituted PAHs by COSMO-RS," Atmos. Environ. **110**, 27–35 (2015).

Paterson, S., Mackay, D., Tam, D., and Shiu, W. Y., "Uptake of organic chemicals by plants: A review of processes, correlations and models," Chemosphere **21**, 297–331 (1990).

Pegoraro, C. N., Chiappero, M. S., and Montejano, H. A., "Measurements of octanol–air partition coefficients, vapor pressures and vaporization enthalpies of the (E) and (Z) isomers of the 2-ethylhexyl 4-methoxycinnamate as parameters of environmental impact assessment," Chemosphere **138**, 546–552 (2015).

Pollack, G. L. and Himm, J. F., "Solubility of xenon in liquid *n*-alkanes: Temperature dependence and thermodynamic functions," J. Chem. Phys. **77**, 3221–3229 (1982).

Pollack, G. L., Himm, J. F., and Enyeart, J. J., "Solubility of xenon in liquid *n*-alkanols: Thermodynamic functions in simple polar liquids," J. Chem. Phys. **81**, 3239–3246 (1984).

Puzyn, T. and Falandysz, J., "Computational estimation of logarithm of *n*-octanol/air partition coefficient and subcooled vapor pressures of 75 chloronaphthalene congeners," Atmos. Environ. **39**, 1439–1446 (2005).

Raevsky, O. A., Grigor'ev, V. J., Raevskaja, O. E., and Schaper, K.-J., "Physicochemical properties/descriptors governing the solubility and partitioning of chemicals in water-solvent-gas systems. Part 1. Partitioning between octanol and air," SAR QSAR Environ. Res. **17**, 285–297 (2006).

Roberts, J. M., "Measurement of the Henry's law coefficient and first order loss rate of PAN in *n*-octanol," Geophys. Res. Lett. **32**, L08803, https://doi.org/10.1029/2004GL022327 (2005).

Rohrschneider, L., "Solvent characterization by gas–liquid partition coefficients of selected solutes," Anal. Chem. **45**, 1241–1247 (1973).

Rumble, J. R., Lide, D. R., and Bruno, T. J., *CRC Handbook of Chemistry and Physics: A Ready-Reference Book of Chemical and Physical Data* (CRC Press; Taylor & Francis, Boca Raton, FL, 2019), https://hbcp.chemnetbase.com/.

Sander, R., "Compilation of Henry's law constants (version 4.0) for water as solvent," Atmos. Chem. Phys. **15**, 4399–4981 (2015).

Schwarzenbach, R. P., Gschwend, P. M., and Imboden, D. M., "Partitioning: Molecular interactions and thermodynamics," in *Environmental Organic Chemistry*, 2nd ed. (John Wiley & Sons, Hoboken, NJ, 2005).

Sepassi, K. and Yalkowsky, S. H., "Simplified estimation of the octanol–air partition coefficient," Ind. Eng. Chem. Res. **46**, 2220–2223 (2007).

Shen, L. and Wania, F., "Compilation, evaluation, and selection of physical–chemical property data for organochlorine pesticides," J. Chem. Eng. Data **50**, 742–768 (2005).

Shoeib, M. and Harner, T., "Characterization and comparison of three passive air samplers for persistent organic pollutants," Environ. Sci. Technol. **36**, 4142–4151 (2002a).

Shoeib, M. and Harner, T., "Using measured octanol-air partition coefficients to explain environmental partitioning of organochlorine pesticides," Environ. Toxicol. Chem. **21**, 984–990 (2002b).

Shoeib, M., Harner, T., Ikonomou, M., and Kannan, K., "Indoor and outdoor air concentrations and phase partitioning of perfluoroalkyl sulfonamides and polybrominated diphenyl ethers," Environ. Sci. Technol. **38**, 1313–1320 (2004).

Staikova, M., Wania, F., and Donaldson, D. J., "Molecular polarizability as a single-parameter predictor of vapour pressures and octanol–air partitioning coefficients of non-polar compounds: A priori approach and results," Atmos. Environ. **38**, 213–225 (2004).

Stenzel, A., Goss, K.-U., and Endo, S., "Prediction of partition coefficients for complex environmental contaminants: Validation of COSMOtherm, ABSOLV, and SPARC," Environ. Toxicol. Chem. **33**, 1537–1543 (2014).

Stephenson, W. K. and Fuchs, R., "Enthalpies of interaction of ketones with organic solvents," Can. J. Chem. **63**, 336–341 (1985a).

Stephenson, W. K. and Fuchs, R., "Enthalpies of hydrogen bond formation of 1-octanol with aprotic organic solvents. A comparison of the solvation enthalpy, pure base, and non-hydrogen-bonding baseline methods," Can. J. Chem. **63**, 342–348 (1985b).

Stephenson, W. K. and Fuchs, R., "Enthalpies of interaction of aromatic solutes with organic solvents," Can. J. Chem. **63**, 2529–2534 (1985c).

Stephenson, W. K. and Fuchs, R., "Enthalpies of interaction of hydroxylic solutes with organic solvents," Can. J. Chem. **63**, 2535–2539 (1985d).

Stephenson, W. K. and Fuchs, R., "Enthalpies of interaction of nitrogen base solutes with organic solvents," Can. J. Chem. **63**, 2540–2544 (1985e).

Strum, D. P. and Eger, E. I., "Partition coefficients for sevoflurane in human blood, saline, and olive oil," Anesth. Analg. **66**, 654–656 (1987).

Su, Y., Lei, Y. D., Daly, G. L., and Wania, F., "Determination of octanol–air partition coefficient (K_{OA}) values for chlorobenzenes and polychlorinated naphthalenes from gas chromatographic retention times," J. Chem. Eng. Data **47**, 449–455 (2002).

Sühring, R., Wolschke, H., Diamond, M. L., Jantunen, L. M., and Scheringer, M., "Distribution of organophosphate esters between the gas and particle phase–model predictions vs measured data," Environ. Sci. Technol. **50**, 6644–6651 (2016).

Taheri, S., Halsey, M. J., Liu, J., Eger, E. I., Koblin, D. D., and Laster, M. J., "What solvent best represents the site of action of inhaled anesthetics in humans, rats, and dogs?," Anesth. Analg. **72**, 627–634 (1991).

Taheri, S., Laster, M. J., Liu, J., Eger, E. I., Halsey, M. J., and Koblin, D. D., "Anesthesia by *n*-alkanes not consistent with the Meyer–Overton hypothesis: Determinations of the solubilities of alkanes in saline and various lipids," Anesth. Analg. **77**, 7–11 (1993).

Tamaru, S., Ono, A., Igura, N., and Shimoda, M., "High correlation between octanol-air partition coefficient and aroma release rate from O/W emulsions under non-equilibrium," Food Res. Int. **116**, 883–887 (2019).

Thomas, E. R. and Eckert, C. A., "Prediction of limiting activity coefficients by a modified separation of cohesive energy density model and UNIFAC," Ind. Eng. Chem. Process Des. Dev. **23**, 194–209 (1984).

Thuens, S., Dreyer, A., Sturm, R., Temme, C., and Ebinghaus, R., "Determination of the octanol–air partition coefficients (K_{OA}) of fluorotelomer alcohols," J. Chem. Eng. Data **53**, 223–227 (2008).

Treves, K., Shragina, L., and Rudich, Y., "Measurement of octanol–air partition coefficients using solid-phase microextraction (SPME)—Application to hydroxy alkyl nitrates," Atmos. Environ. **35**, 5843–5854 (2001).

Tse, G. and Sandler, S. I., "Determination of infinite dilution activity coefficients and 1-octanol/water partition coefficients of volatile organic pollutants," J. Chem. Eng. Data **39**, 354–357 (1994).

Ulrich, N., Endo, S., Brown, T., Bronner, G., Abraham, M. H., and Goss, K.-U., UFZ-LSER Database V 3.2.1 [Internet], Helmholtz Centre for Environmental Research-UFZ, Leipzig, Germany, 2017, http://www.ufz.de/lserd.

US EPA, Estimation Programs Interface SuiteTM v.4.11, United States Environmental Protection Agency, Washington, DC, 2012, https://www.epa.gov/tsca-screening-tools/epi-suitetm-estimation-program-interface.

Vikas and Chayawan, "Single-descriptor based quantum-chemical QSPRs for physico-chemical properties of polychlorinated-dibenzo-*p*-dioxins and -dibenzo-furans (PCDD/Fs): Exploring the role of electron-correlation," Chemosphere **118**, 239–245 (2015).

Vuong, Q. T., Thang, P. Q., Ohura, T., and Choi, S.-D., "Determining subcooled liquid vapor pressures and octanol-air partition coefficients for chlorinated and brominated polycyclic aromatic hydrocarbons based on gas chromatographic retention times: Application for gas/particle partitioning in air," Atmos. Environ. **229**, 117461 (2020).

Wang, Q., Zhao, H., Wang, Y., Xie, Q., Chen, J., and Quan, X., "Determination and prediction of octanol-air partition coefficients for organophosphate flame retardants," Ecotoxicol. Environ. Saf. **145**, 283–288 (2017).

Wang, T., Han, S., Yuan, B., Zeng, L., Li, Y., Wang, Y., and Jiang, G., "Summer–winter concentrations and gas-particle partitioning of short chain chlorinated paraffins in the atmosphere of an urban setting," Environ. Pollut. **171**, 38–45 (2012).

Wang, Z.-Y., Zeng, X.-L., and Zhai, Z.-C., "Prediction of supercooled liquid vapor pressures and *n*-octanol/air partition coefficients for polybrominated diphenyl ethers by means of molecular descriptors from DFT method," Sci. Total Environ. **389**, 296–305 (2008).

Wania, F. and Dugani, C. B., "Assessing the long-range transport potential of polybrominated diphenyl ethers: A comparison of four multimedia models," Environ. Toxicol. Chem. **22**, 1252–1261 (2003).

Wania, F., Lei, Y. D., and Harner, T., "Estimating octanol–air partition coefficients of nonpolar semivolatile organic compounds from gas chromatographic retention times," Anal. Chem. **74**, 3476–3483 (2002).

Weschler, C. J. and Nazaroff, W. W., "SVOC partitioning between the gas phase and settled dust indoors," Atmos. Environ. **44**, 3609–3620 (2010).

Wilcock, R. J., Battino, R., Danforth, W. F., and Wilhelm, E., "Solubilities of gases in liquids. II. The solubilities of He, Ne, Ar, Kr, O_2, N_2, CO, CO_2, CH_4, CF_4, and SF_6 in *n*-octane, 1-octanol, *n*-decane, and 1-decanol," J. Chem. Thermodyn. **10**, 817–822 (1978).

Wilhelm, E. and Battino, R., "Precision methods for the determination of the solubility of gases in liquids," CRC Crit. Rev. Anal. Chem. **16**, 129–175 (1985).

Williams, A. J., Grulke, C. M., Edwards, J., McEachran, A. D., Mansouri, K., Baker, N. C., Patlewicz, G., Shah, I., Wambaugh, J. F., Judson, R. S., and Richard, A. M., "The CompTox chemistry Dashboard: A community data resource for environmental chemistry," J. Cheminf. **9**, 61 (2017).

Xiao, H., Li, N., and Wania, F., "Compilation, evaluation, and selection of physical–chemical property data for α-, β-, and γ-hexachlorocyclohexane," J. Chem. Eng. Data **49**, 173–185 (2004).

Xu, H.-Y., Zou, J.-W., Yu, Q.-S., Wang, Y.-H., Zhang, J.-Y., and Jin, H.-X., "QSPR/QSAR models for prediction of the physicochemical properties and biological activity of polybrominated diphenyl ethers," Chemosphere **66**, 1998–2010 (2007).

Xu, S., Kozerski, G., and Mackay, D., "Critical review and interpretation of environmental data for volatile methylsiloxanes: Partition properties," Environ. Sci. Technol. **48**, 11748–11759 (2014).

Xu, S. and Kropscott, B., "Evaluation of the three-phase equilibrium method for measuring temperature dependence of internally consistent partition coefficients (K_{OW}, K_{OA}, and K_{AW}) for volatile methylsiloxanes and trimethylsilanol," Environ. Toxicol. Chem. **33**, 2702–2710 (2014).

Xu, S. and Kropscott, B., "Octanol/air partition coefficients of volatile methylsiloxanes and their temperature dependence," J. Chem. Eng. Data **58**, 136–142 (2013).

Xu, S. and Kropscott, B., "Method for simultaneous determination of partition coefficients for cyclic volatile methylsiloxanes and dimethylsilanediol," Anal. Chem. **84**, 1948–1955 (2012).

Yalkowsky, S. H., Dannenfelser, R.-M., Myrdal, P., and Simamora, P., "Unified physical property estimation relationships (Upper)," Chemosphere **28**, 1657–1673 (1994a).

Yalkowsky, S. H., Myrdal, P., Dannenfelser, R.-M., and Simamora, P., "Upper II: Calculation of physical properties of the chlorobenzenes," Chemosphere **28**, 1675–1688 (1994b).

Yaman, B., Dumanoglu, Y., and Odabasi, M., "Measurement and modeling the phase partitioning of organophosphate esters using their temperature-dependent octanol–air partition coefficients and vapor pressures," Environ. Sci. Technol. **54**, 8133 (2020).

Yang, M., Li, Y.-F., Qiao, L.-N., and Zhang, X.-M., "Estimating subcooled liquid vapor pressures and octanol-air partition coefficients of polybrominated diphenyl ethers and their temperature dependence," Sci. Total Environ. **628-629**, 329–337 (2018).

Yao, Y., Harner, T., Ma, J., Tuduri, L., and Blanchard, P., "Sources and occurrence of Dacthal in the Canadian atmosphere," Environ. Sci. Technol. **41**, 688–694 (2007).

Yaws, C. L., *Solubility Parameters and Liquid Molar Volumes–Organic Compounds* (Knovel, New York, 2012), https://app.knovel.com/hotlink/itble/rcid:kpYTPCHE02/id:kt0078OOJ1/yaws-thermophysical-properties/yaws-therm-solubility.

Yuan, J., Yu, S., Zhang, T., Yuan, X., Cao, Y., Yu, X., Yang, X., and Yao, W., "QSPR models for predicting generator-column-derived octanol/water and octanol/air partition coefficients of polychlorinated biphenyls," Ecotoxicol. Environ. Saf. **128**, 171–180 (2016).

Zeng, X.-L., Zhang, X.-L., and Wang, Y., "QSPR modeling of *n*-octanol/air partition coefficients and liquid vapor pressures of polychlorinated dibenzo-*p*-dioxins," Chemosphere **91**, 229–232 (2013).

Zhang, N., Yang, Y., Liu, Y., and Tao, S., "Determination of octanol-air partition coefficients and supercooled liquid vapor pressures of organochlorine pesticides," J. Environ. Sci. Health B **44**, 649–656 (2009).

Zhang, Q., Zhao, H., Chen, J., and Liang, X., "Correlation between octanol-air partition coefficients and retention parameters of polychlorinated biphenyls on gas chromatographic columns," Se Pu **23**, 441 (2005), https://pubmed.ncbi.nlm.nih.gov/16350783/.

Zhang, X., Schramm, K.-W., Henkelmann, B., Klimm, C., Kaune, A., Kettrup, A., and Lu, P., "A method to estimate the octanol–air partition coefficient of semivolatile organic compounds," Anal. Chem. **71**, 3834–3838 (1999).

Zhang, X., Sühring, R., Serodio, D., Bonnell, M., Sundin, N., and Diamond, M. L., "Novel flame retardants: Estimating the physical–chemical properties and environmental fate of 94 halogenated and organophosphate PBDE replacements," Chemosphere **144**, 2401–2407 (2016).

Zhao, H., Chen, J., Quan, X., Qu, B., and Liang, X., "Octanol–air partition coefficients of polybrominated biphenyls," Chemosphere **74**, 1490–1494 (2009).

Zhao, H., Xie, Q., Tan, F., Chen, J., Quan, X., Qu, B., Zhang, X., and Li, X., "Determination and prediction of octanol–air partition coefficients of hydroxylated and methoxylated polybrominated diphenyl ethers," Chemosphere **80**, 660–664 (2010).

Zhao, H., Zhang, Q., Chen, J., Xue, X., and Liang, X., "Prediction of octanol-air partition coefficients of semivolatile organic compounds based on molecular connectivity index," Chemosphere **59**, 1421–1426 (2005).

Zhu, T., Li, J., Hawkins, G. D., Cramer, C. J., and Truhlar, D. G., "Density functional solvation model based on CM2 atomic charges," J. Chem. Phys. **109**, 9117–9133 (1998).

Zou, J.-W., Jiang, Y.-J., Hu, G.-X., Zeng, M., Zhuang, S.-L., and Yu, Q.-S., "QSPR/QSAR studies on the physicochemical properties and biological activities of polychlorinated biphenyls," Acta Phys.-Chim. Sin. **21**, 267–272 (2005).